NATIONAL ADVISORY COMMITTEE
FOR AERONAUTICS

TECHNICAL NOTE 2634

EVALUATION OF THREE METHODS FOR DETERMINING DYNAMIC

CHARACTERISTICS OF A TURBOJET ENGINE

By Gene J. Delio

Lewis Flight Propulsion Laboratory
Cleveland, Ohio

NACA

1K

NATIONAL ADVISORY COMMITTEE FOR AERONAUTICS

TECHNICAL NOTE 2634

EVALUATION OF THREE METHODS FOR DETERMINING DYNAMIC

CHARACTERISTICS OF A TURBOJET ENGINE

By Gene J. Delio

SUMMARY

Transient data resulting from approximate step and sinusoidal disturbances of fuel flow were obtained on a turbojet engine operated at one constant simulated altitude and flight condition. The data were analyzed to evaluate various procedures for obtaining engine dynamic characteristics.

Three of the more common methods of analysis chosen for study gave the following information: (1) Transient analysis yielded the basic dynamic characteristics with minimum running time and computation. (2) Fourier analysis yielded engine frequency spectra beneficial in control synthesis, but was sensitive to instrumentation and approximation errors. Computation time was excessive. (3) AC analysis yielded the additional high-frequency characteristics of the engine at the expense of longer running time and moderate amount of computation.

With the use of these three methods, accurate engine dynamics data could be obtained for use in high gain controls only if the source impedances and engine nonlinearities were considered. Also, under certain restrictions and approximations, functional relationships could be used to derive turbojet engine transfer functions.

INTRODUCTION

Dynamical systems are, in general, described and defined by differential equations. In many cases, the experimental determination of these equations and their utilization in analyses are very awkward or difficult. If, as in the case of the turbojet engine, the dynamics can be assumed to be essentially linear, alternative more useful representations can be used.

The Fourier integral theorem is the basic mathematical technique which translates the dynamical behavior of linear systems from the time domain to the frequency domain and vice versa. In the time domain, the

system dynamics are described by the time response to transient inputs, such as a step or a pulse. The frequency domain is characterized by sinusoidal response (amplitude and phase) to a sinusoidal input (reference 1, ch. 10).

There is thus a choice as to the experimental techniques to be used in investigating turbojet engine dynamics. The use of transient inputs gives directly the time domain information which is the most direct description of the quality and nature of the system. The use of sinusoidal inputs gives directly the frequency response; and this form is often most useful in analyses, such as closed loop control system analyses, stability tests, and effects of random inputs (reference 2, ch. 4).

For ideal systems the various experimental techniques, used in conjunction with Fourier analysis to convert from one domain to the other, would give identical results. If one of the standard inputs is difficult to obtain, that input which is obtained with facility can be used. The response to this input can be translated, theoretically, to the response to the desired input (reference 3, p. 37, and reference 1, ch. 10). Considerations of deviations from linearity, accuracy of instrumentation, noise or "hash," as well as the practical considerations of limitations of running time and of ease of obtaining and processing data, however, separate the various methods as to their applicability.

The object of this report is to provide a detailed comparison of three methods of analysis, carried out at the NACA Lewis laboratory, in order to make possible a choice of a suitable method of determining engine dynamic characteristics. Data resulting from an approximate step function input are analyzed by two methods: (1) Functional relationships are observed directly from the data which lead to differential equations describing the data, and (2) Fourier analysis of the data is performed. A third method uses data resulting from sinusoidal disturbances to experimentally define the frequency response functions. The Fourier transform is used to show the essential equivalence of the methods and to compare them. The limitations of each method of analysis are discussed with respect to the accuracy of results, ease of obtaining and processing data, effect of engine supply sources on data, and economical use of engine and test facilities.

APPARATUS AND PROCEDURE

Engine Installation

Engine. - A turbojet engine was mounted on a wing section which spanned the test section of the NACA Lewis altitude wind tunnel. The

altitude and flight Mach number were simulated in the following manner. Air from a climatic control source was applied to the engine through a ram pipe. The engine exhausted into the altitude wind tunnel, which approached an infinite sink. The wind tunnel static pressure and engine inlet total pressure and total temperature were a measure of simulated flight speed and altitude.

The main components of the engine used in this investigation consisted of an eleven-stage axial-flow compressor, eight through-flow combustors, a single-stage turbine, and a fixed-area exhaust nozzle. A sketch of this engine is shown in figure 1.

Fuel system. - The fuel distribution system was of standard design, except for the fuel metering valve. This valve was designed to maintain a fixed flow rate for each valve position independent of the fuel inlet pressure and combustion chamber pressure. The constant flow rate was maintained by regulating the pressure drop across the fuel valve with a regulatory bypass connected across the fuel valve.

An independent source of voltage was used to regulate fuel flow by feeding the signal into a positional servomotor which was coupled to the fuel valve through suitable gear reduction. Because of the characteristics of this fuel flow controller, a linear relationship existed between the fuel valve position and input signal.

The DC voltage level determined the engine operating point, and a switching of the DC levels produced approximate step changes in fuel flow. A variable frequency voltage generator produced a sinusoidal voltage of required amplitude and frequency which was superimposed on a DC voltage level. In this manner, a sinusoidally varying fuel flow was impressed upon the engine about the desired operating level.

Instrumentation

All quantities measured were recorded using instrumentation with the following characteristics: (1) linear phase shift and flat frequency response, (2) sensing elements with suitable dynamic response and linear electrical outputs, and (3) signal amplification about an arbitrary operating point. Those quantities whose characteristics were definitely dynamic were recorded on an oscillograph to obtain the wave form of the transient, while the initial and final equilibrium points were recorded by photographing an instrument panel.

Instrumentation for transient data. - The signal outputs of the various sensing elements were generally too weak to be recorded directly and suitable amplifying equipment was therefore necessary.

The instrumentation consisted basically of a multichannel recorder, associated amplifiers, and sensing element for each channel. The two basic recording systems are shown in figure 2.

Engine speed was sensed by a small DC motor coupled directly to the compressor shaft. The motor was used as a generator to convert the rotational speed of the engine into an electrical signal which was fed into a low-pass, "constant k," filter (reference 4, p. 329) to remove commutator ripple and hash. The resultant signal was amplified and recorded. A block diagram of this system is shown in figure 2(a).

Gas pressures were sensed by commercially available transducers which incorporated bellows mechanically connected to a bonded strain gage bridge having four active gages. The bridge unbalance was fed into a strain amplifier and recorded. The sensing elements (pressure transducer and connecting tubing) were designed for the desired pneumatic behavior (reference 5). A block diagram of the system is shown in figure 2(b).

Fuel flow was measured with a differential pressure transducer which measured the pressure drop across an orifice. For fuel flow changes of the order of 1 percent, the pressure drop was considered to vary linearly with the fuel flow through the orifice. Fuel valve position was converted into an electrical signal by a potentiometer mechanically coupled to the fuel valve.

Instrumentation for steady-state data. - The photopanel recording of equilibrium points was accomplished with a conventional instrument panel and a camera rigidly mounted to avoid mechanical vibration. Pressures were measured by manometers, engine speed by a chronometric tachometer, and fuel flow by rotameters.

Recording technique. - When the engine was in equilibrium at the initial conditions, and prior to the proposed transient, steady-state information was recorded at the photopanel. Immediately following the transient, information at the photopanel was again recorded, thereby providing calibration for each trace of the oscillograph. Linearity was assumed for the calibration.

Generally, two methods of calibration were used, depending on the type of transient involved. For a transient in which the initial and final steady-state values differed, calibration was obtained by using values obtained from the steady-state instrumentation. For a transient in which the initial and final values were essentially the same, a calibration was obtained by recording steady-state values for two different engine conditions while maintaining the instrumentation gain settings constant. The oscillograph traces were then calibrated using the scale gradient thus obtained and the initial steady-state recording.

Procedure

The turbojet engine was operated at a constant altitude of 15,000 feet and an inlet Mach number of 0.22 for all conditions reported herein. Step disturbances in the fuel valve setting were made throughout the engine speed range. The magnitude of these disturbances resulted in speed changes of 1 percent rated sea-level speed ($0.01\ N_r$). In addition, step disturbances in fuel valve position were introduced about an average operating point of $0.94\ N_r$ that resulted in speed changes of $0.02\ N_r$, $0.04\ N_r$, and $0.08\ N_r$.

Sinusoidal disturbances in fuel flow were impressed upon the engine in the neighborhood of three operating points: $0.88\ N_r$, $0.94\ N_r$, and $0.98\ N_r$. At these speeds the amplitude of the fuel flow disturbances was adjusted to a value sufficient to cause a change of $\pm0.01\ N_r$ at zero frequency for the three operating points investigated. In addition, at $0.94\ N_r$ the amplitude of the sinusoidal fuel flow was adjusted to produce engine speed changes of $\pm0.02\ N_r$ and $\pm0.04\ N_r$ at zero frequency.

ANALYSIS

Step function changes are useful test disturbances in determining the nature of response. They are easily applied and often approximate certain operating conditions. The condition most controlled systems are most likely to encounter in operation, however, is one in which the input is arbitrarily varied; and the response of this system to such a random disturbance may be considered as a linear summation of sinusoidal functions over an appropriate frequency range. For the latter case, a sinusoidal disturbance of various frequencies experimentally defines system performance (reference 1, ch. 4).

Functional Relationships

When a turbojet engine has a step input disturbance in fuel flow, the responses indicate that the engine is a single capacity system. Thus, differential equations can be easily derived that fit the experimental response curves (references 6 and 7). (All symbols used are defined in appendix A.)

These equations are derived in appendix B for a turbojet engine with 3 degrees of freedom. The independent variables, or inputs, considered are: primary engine fuel flow, reheat fuel flow, and exhaust nozzle area. The final equations which describe engine dynamic behavior

are in transfer function form, from which it is possible to transform to differential equation form, or frequency response form.

Engine speed. - From the basic assumptions and mathematical develop-ment shown in appendix B, the solution of the differential equation describing engine speed response to a step disturbance in fuel flow is

$$\Delta N = K_{nW} \Delta W \left(1 - e^{-t/\tau} \right)$$
(1)

The speed response is exponential in nature between initial and final equilibrium points. The speed gain K_{nW} is a measure of sensitivity and is the speed change due to a change in fuel flow. The engine time constant τ is a measure of engine acceleration and is the time for the engine to accelerate to 63 percent of the final speed change. A theoretical speed response to a step change in fuel flow is shown in figure 3(a).

An experimental speed response resulting from an approximate step change in fuel flow is shown in figure 4. Examination shows some departure from a theoretical first-order response. Although the dominant lag in engine speed caused by the rotor inertia is present, additional lags appear at the start of the transient. These lags are much shorter than the speed lag and may be attributed to the following causes: (1) instrumentation lag, including the lag introduced by the speed signal filter; (2) fuel system lag, or the time required for the fuel flow to increase to the flow required at the prescribed fuel valve setting; and (3) combustion lag, or the time needed for combustion equilibrium to be reached.

The preceding lags appear as a chain of series connected lags which can be considered as sequenced systems represented by lumped parameters (reference 8, ch. 7). These lags can be considered dead time in total effect. Usable results are obtained by replacing the chain with a system whose response to a step disturbance is represented by dead time plus a first-order response. As shown in figure 4, the speed response was extrapolated exponentially to the initial steady-state value, and the difference in time between this value and the initiation of the transient (time of fuel valve position change) is considered dead time.

Compressor-discharge total pressure. - The response of the compressor-discharge total pressure to an approximate step change in fuel flow (fig. 4) is seen to be composed of two parts. There·is a sudden pressure rise due to a fuel flow change at constant speed, and an exponential rise due to speed change at constant fuel flow. With the use of the basic assumptions and mathematical development in appendix B, the transient response of figure 4 can be described by

$$\Delta P_c = K_{p_c w} \Delta W \left[1 - (1-d)e^{-t/\tau} \right] \qquad (2)$$

The pressure gain $K_{p_c w}$ is the total change in pressure due to a fuel flow change, and the initial rise ratio d is the ratio of the initial pressure rise at constant speed to the total change in pressure. A theoretical pressure response to a step change in fuel flow is shown in figure 3(b).

As with the speed response, the pressure response was assumed to begin at the time coinciding with the extrapolated initial point of the speed response. The initial rise is assumed to occur at this time.

Fourier Representation

Any time excitation or response function may be specified in terms of its frequency components according to the methods of Fourier. Consequently, it is possible to deal with the dynamics of linear systems entirely in the frequency domain (reference 2, ch. 10).

The useful part of the recordings (fig. 4) where the function is of bounded variation, and starts and ends in steady state, can be resolved by the Fourier theorem into individual harmonic oscillations. From appendix C, the frequency response function is

$$KG(i\omega) = \frac{\int_0^T \cos \omega t \, dy(t) - i \int_0^T \sin \omega t \, dy(t)}{\int_0^T \cos \omega t \, dx(t) - i \int_0^T \sin \omega t \, dx(t)} \qquad (C5)$$

The two types of integral can be evaluated by digital computers for each harmonic frequency ω in the form

$$KG(i\omega) = \frac{A(\omega) - iB(\omega)}{C(\omega) - iD(\omega)} \qquad (C10)$$

from which expression the amplitude and phase angle can be determined in well-known fashion (appendix C).

The validity of this method of transposing from the time domain to the frequency domain can be checked by the following functions, which are typical of engine response data. Given an input function

$$I(t) = 1 + 0.1 \, e^{-t/8}$$

and an output function

$$O(t) = 1 - e^{-\frac{(t-0.4)}{4}}$$

the theoretical transfer loci, assuming each function to result from a step input, can be plotted for both functions (fig. 5), and the transfer loci relating the output to the input are shown in figure 6. Also plotted are the results of Fourier analysis of both functions for 24 discrete frequencies. At low frequencies, the approximation is practically exact; and at high frequencies the approximation yields an error of 20 percent in the phase angle but negligible error in magnitude.

Frequency Response

If a system is linear or nearly so, the steady-state frequency response uniquely describes its characteristics. The application of frequency response analysis to physical systems does not have to distinguish between lumped or distributed parameters (reference 9, pp. 120-123).

The frequency response functions which best fit the experimental data are (reference 1, ch. 8): for speed

$$KG(i\omega) = \frac{K_{nw}}{1+\tau i\omega}$$

and for pressure

$$KG(i\omega) = K_{p_c w} \frac{(1+d\tau i\omega)}{1+\tau i\omega}$$

These frequency spectra may be graphically represented (figs. 7(a) and 7(b)) by plotting the logarithm of the output magnitude, and the phase, as functions of the logarithm of the frequency. Typical data obtained by the sinusoidal variation of the fuel valve of a turbojet engine are shown in figure 8.

RESULTS

Several dynamic characteristics of a turbojet engine were determined experimentally using two operational inputs. The transient fuel flow input was assumed a step input for the responses from which the coefficients of the differential equations were determined, and the actual fuel flow input was used in Fourier analysis. A sinusoidal input was used in directly determining the frequency response. All gains, time constants, and frequencies have been made dimensionless using the factors given in the symbol list (appendix A).

Coefficients of differential equations. - The experimental indicial responses obtained by approximate step disturbances in the fuel valve setting were analyzed to yield the coefficients of the differential equations describing the behavior of engine speed and compressor-discharge total pressure (equations (1) and (2)). The speed gain K_{nW}, pressure gain K_{p_cW}, and initial rise ratio d are shown in figure 9 as functions of engine speed. The variation of engine time constant τ with engine speed is shown in figure 10. The measured time constant, as discussed in the analysis section, is an approximation of engine speed lag and does not include the higher-order effects caused by additional lags.

The results of increased magnitude of step disturbances applied about an average speed of 0.94 N_r are listed in table I.

Fourier representation. - The particular indicial responses (fig. 4) were subjected to Fourier analysis. The transfer loci of pressure, fuel flow, and speed for an assumed step disturbance are plotted in figure 11. The particular gains are made arbitrary at zero frequency for illustrative purposes only.

The frequency response function relating speed to fuel flow is obtained using equations (C7) and (C8) of appendix C, and is graphically defined in figure 12. Similarly, the frequency response function relating compressor-discharge total pressure to fuel flow is illustrated in figure 13. Figure 4 represents indicial responses caused by an increase in fuel valve setting resulting in a final speed change of 0.08 N_r about an average operating point of 0.94 N_r. A Fourier analysis of these data yields an engine time constant τ/τ_1 of 0.67, and an initial rise ratio d of 0.80. The engine time constant was determined by the intersection of the two asymptotes (fig. 12), and the initial rise ratio was determined by the asymptote in the high-frequency region (fig. 13).

Frequency response. - Although frequency spectra were obtained from time functions with the use of the Fourier integral, the frequency spectra are directly obtainable using sinusoidal inputs. Typical frequency spectra

thus obtained are illustrated in figures 14 and 15. The results of AC
analysis for three operating points are listed in table II and the effect
of increased amplitude of disturbance is illustrated in table III. The
frequency responses of speed to fuel valve setting for the three ampli-
tudes are illustrated in figure 16.

DISCUSSION

Quantitative information characterizing engine dynamic responses
was obtained by three methods using two common input disturbances.
The methods are discussed for their relative accuracies, and the com-
puting and engine times required.

Transient Analysis

Although the solutions of differential equations describing
physical systems give an understanding of its performance, the method
is difficult to apply to higher-order systems without undue idealiza-
tion. If the idealized engine can be represented by a single capacity
system, indicial responses can yield directly the required coefficients
of the differential equations. If instrumentation, fuel system, com-
bustion lags, and source impedances are negligible, the dominant lag
and sensitivities can be determined directly from the traces (fig. 4).

The assumptions of appendix B are valid only for small inputs.
Higher-order effects magnified by large inputs must be considered.
As an example, the speed trace of figure 4 includes what is considered
to be dead time, lasting from the initiation of the transient to the
extrapolated point of initial speed response. Another consideration is
the reactance of the engine with the fuel and air supplies. The
measured time lags and engine gains include the effect of source
impedances; and with the use of the equations developed in appendix B,
idealized time lags and engine gains may be calculated which assume
zero impedance sources (fully regulated air and fuel supplies).   ·

A series of indicial responses will quickly bracket the engine
operating range and yield the sensitivities and lags for each operating
point tested. Although engine operating time and data reduction time
are at a minimum, the following limitations must be considered.

Engine nonlinearity is illustrated in table I in which increased
magnitudes of disturbance yielded decreased time lags and decreased
values for the initial rise ratio. Part of the decrease in engine
time constant can be explained by the engine reactance with the air
supply source (equation (B7) of appendix B). However, the major part
of the decrease is attributed to the variation of the engine time

constant with speed equilibrium point. For the range above 0.88 N_r the effective engine time constant is lower at the initiation of the acceleration, than the effective time constant at the final equilibrium point.

The initial rise ratio d decreases with increased amplitude disturbance (table I). Reaction between engine and supply sources would cause increased values (equation (B20) of appendix B). For the test procedure used, the increasing magnitudes were accomplished about an average point 0.94 N_r; that is, the larger steps started progressively at lower speeds and ended at higher speeds. From figure 9, it is seen that the initial rise ratio decreases with decreasing speed. Therefore, the initial pressure rise due to fuel flow change occurs at progressively lower speeds for large steps, resulting in lower initial pressure rise ratios.

Although it is desired to use disturbance magnitudes that are as small as possible to closely approximate the idealized engine, instrumentation sensitivity and error place a lower limit on the usable input magnitudes. With instrumentation sufficiently sensitive to record engine perturbations and turbulence, the input magnitudes can be reduced only to the point at which the responses approach the order of the inherent randomness of the engine variables.

Fourier Analysis

The frequency spectra of a turbojet engine are often used as an aid in the synthesis of engine controls, and transformation from the frequency domain to the time domain is unnecessary (reference 2, ch. 7). In the frequency domain, stability and effectiveness can be deduced from simple plots in a method which lends itself to the use of analytical and experimental data, or to combinations of both. Although step function inputs can be used to judge the quality of response, time responses are not essential for synthesis.

In an effort to keep engine operating time at a minimum, and yet produce engine frequency spectra, Fourier analysis was performed on an input and the corresponding output. The resultant magnitude and phase spectra are shown in figures 11 and 12. Although engine and equipment times are at a minimum, computing and analysis times are at a maximum.

The increasing amplitude ratio in the low-frequency region is thought to be a perturbation outside the engine system, and thus not attributable to engine dynamics. As can be seen from figure 11, the transfer locus of measured fuel flow to an assumed step input of fuel flow shows the presence of a low-frequency component. Detailed investigation of the data of figure 4, which were subjected to Fourier analysis,

shows that fuel flow reaches a maximum quickly, slowly decreases to a
minimum, then gradually increases again with time. The frequency
spectrum relating pressure to fuel flow shows similar behavior.

The transfer locus of speed to an assumed step disturbance
(fig. 11) shows a departure from a first-order system. Examination
of figure 4 shows a time delay starting at the initial point of the
transient. This delay time, or dead time, masks the lag time of the
speed response; and the engine appears as a higher-order system.
However, the frequency spectrum relating speed to actual fuel flow
(fig. 12) consists of a magnitude spectrum indicating a first-order
system, and a phase spectrum indicating a higher-order system. Thus,
the delay time is evidenced as additional phase shift. This indicates
that the engine is not a minimal phase system (reference 9, pp. 120-123).
Both the magnitude and phase spectra are necessary to describe engine
dynamic behavior. For example, unstable combustion during acceleration
introduces space derivatives causing additional phase shifts. Especially
for large disturbances of fuel flow, engine behavior departs from that
of an idealized engine (lumped constant, minimal phase); and engine
behavior is described by a distributed parameter system which is not of
minimal phase.

Comparison of figures 12 and 14 with figure 7(a) indicates that the
speed response to actual fuel flow is exponential in nature and that the
engine is primarily a first-order system. The comparison of figure 13
and 15 with figure 7(b) shows that the pressure response to actual fuel
flow is of a lag nature (reference 1, p. 265). The high-frequency
scatter in figures 12 and 13 is due to the nature of the approximation
used (appendix B) in the Fourier analysis. An increase in the number
of ordinates for approximating the transient recordings would have
reduced the high-frequency scatter. As shown by figures 5 and 6 this
particular procedure for Fourier analysis is valid for functions that
are continuous and differentiable for $t \geqq 0$ (appendix C); however, it
is very sensitive to perturbation and noise contained in the actual
responses, and to the number of ordinates used. The number of ordinates
per second of transient time must be kept as high as practical.

Frequency Response

Because frequency spectra are useful in visualizing the dynamic
characteristics of a physical system, sinusoidal disturbances were
applied to the turbojet engine. The frequency of oscillation was
increased until readability of data was limited by instrumentation.
Figures 14 and 15 are plots of the frequency response of speed, pressure,
and fuel flow to fuel valve position.

The magnitude $K|G(i\omega)|$ is composed of a frequency invariant part K and a frequency variant part $|G(i\omega)|$. For this investigation, K is the engine gain relating the fuel valve position with the speed, pressure, and fuel flow; $G(i\omega)$ represents that part which varies with frequency and it is a function of the energy storage of the engine. Figures 14 and 15 have been normalized by dividing the magnitude by K and therefore apply only to the frequency variant portions of the magnitude.

In figure 14 the first corner frequency of the speed response curve characterizes the engine time constant τ. The 45° slope defines a first-order system, and the second corner frequency is due to the lag in the fuel system. Information contained in the higher-frequency range demonstrates the nature of the fuel system. If this response is approximated by the drawing of a 45° slope through most of the data points, an equivalent time constant τ_f results. It is seen that the fuel system source impedance is reflected in the speed response. Figure 15 shows a similar effect.

The effect of amplitude of disturbance is illustrated by figure 16. Increased amplitude yields decreased values of engine time constants. Although the magnitude spectrum indicates a lumped constant system, the phase spectrum indicates additional phase shift which can result from dead time. Thus, the engine is not a minimal-phase system. Because the amplitude ratio increases with amplitude of disturbance at a given frequency, it is possible that there exists a dead band which would account for this effect for, in the extreme case, a disturbance amplitude entirely within the dead band would result in zero output amplitude.

Engine frequency response appears to yield the same information as transient analysis and Fourier analysis, especially in the low-frequency domain. The method of frequency response yields additional high-frequency data, such as fuel system lag, within the limitation of the type of instrumentation used. The nature of nonlinearity such as dead time is also revealed. Engine and equipment operating times, however, are at a maximum.

The effect of excessive lags in a control loop for an engine may result in instability if the loop gain is too high. Control systems become more oscillatory as the loop gain is increased, and the oscillation can be sustained indefinitely or increased with time. Although stability criteria may indicate for idealized second-order or first-order systems that gain can be increased indefinitely without instability, in physical systems this is impossible. Instability will always result because of factors neglected in the idealization. If Nyquist's criterion did indicate the presence of roots with positive real parts

(reference 1, p. 175), the oscillations resulting from a small disturbance
would not, in a physical system, increase indefinitely in magnitude.
Under these circumstances, the oscillations will increase in magnitude
until the apparatus destroys itself, or until nonlinearities limit the
oscillations to some finite magnitude.

A recording of controlled engine acceleration using a high gain
controller in a speed - fuel-flow loop is shown in figure 17. The block
diagram of the control loop is shown in figure 18. Fuel system lag,
coupled with combustion delay time and instrumentation lag, was suffic-
ient to reduce the gain margin to approximately 26 decibels (fig. 14).
In figure 17 speed is controlled by fuel flow, with an upper limit on
the fuel valve opening to prevent compressor stall and surge. As top
speed is approached, the control gain is suddenly increased in an
effort to increase control effectiveness. The resultant loop gain, in
the vicinity of 26 decibels, was sufficient to cause oscillatory fuel
flow at a frequency in the spectral region of the fuel system time
constant indicated in figure 14.

Comparison of Methods

The time constant which resulted from frequency response analysis
was consistently higher than the time constant which resulted from
transient analysis. Because of the approximation used in transient
analysis, the time constant did not include higher-order effects;
whereas, the apparent time constant which resulted from frequency
response analysis was affected by the nearness of the equivalent fuel
system time constant (fig. 14). Similarly the values for initial rise
ratio were decreased values because of the nearness of the equivalent
fuel system time constant (figs. 14 and 15). A comparison is made in
table IV.

Increased amplitude disturbances yielded results which demonstrated
engine nonlinearity (table III). For increased magnitudes of distur-
bances, the frequency response method again yielded values of engine
time constant that were higher than those obtained from transient
analysis (table I). Thus, both methods of analysis showed similar
nonlinear effects for evaluating the engine time constant. However,
both methods of analysis showed dissimilar nonlinear effects for
evaluating the initial pressure rise ratio. A comparison is made in
table V.

Fourier analysis resulted in values of engine dynamic character-
istics comparable with those obtained by AC analysis but higher than
those obtained from transient analysis. As explained previously,
transient analysis used an approximate method which did not include
higher-order effects. A comparison is made in table VI.

A comparison of the three methods for determining the speed response to fuel flow disturbances in the frequency domain is shown in figure 19.

SUMMARY OF RESULTS

The three methods of analysis applied to turbojet engines produced engine dynamics data usable to varying degrees in control synthesis. The choice of method is dependent on the engine and calculating times available, degree of accuracy desired, type of instrumentation used, and the application of the results.

The following results were obtained from the evaluation of the analyses:

1. Transient analysis yielded the basic engine time constant and various engine gains with minimum engine, computation, and equipment operating time. Under the limitation of the instrumentation and recording system, however, transient analysis did not yield the rapid response or high-frequency characteristics of the engine and its associated systems.

2. Fourier analysis of engine transient data produced engine frequency spectra beneficial in control synthesis. However, this method was sensitive to instrumentation and approximation errors. Calculating time was excessive. It would be especially excessive if the approximation accuracy were increased in an effort to obtain high-frequency data.

3. AC analysis yielded high-frequency information, such as fuel system lags, at the expense of engine and equipment operating time and of calculating time. This type of information was necessary in high-speed and high gain control systems.

4. Only if the source impedance of the test facilities and the nonlinearities of the turbojet engine were considered could accurate engine dynamics data be obtained for use in high gain controls.

5. Under certain restrictions and approximations, functional relationships could be used to derive turbojet engine transfer functions which fit the experimental data and which are easily manipulated in control loop synthesis.

Lewis Flight Propulsion Laboratory
    National Advisory Committee for Aeronautics
        Cleveland, Ohio, November 26, 1951

APPENDIX A

SYMBOLS

The following symbols are used in this report:

A   exhaust nozzle area, sq ft

A,B,C,D   constants

d   initial pressure rise ratio due to step change in fuel flow

at constant A, W_2, and P; $\dfrac{\left(\dfrac{\partial P_c}{\partial W}\right)_N}{K_{p_c w}}$

e   base of natural logarithms

f   initial pressure rise ratio due to step change in reheat fuel

flow at constant A, W, and P; $\dfrac{\left(\dfrac{\partial P_c}{\partial W_2}\right)_N}{K_{p_c w_2}}$

g   initial pressure rise ratio due to a step change in area at

constant W, W_2, and P; $\dfrac{\left(\dfrac{\partial P_c}{\partial A}\right)_N}{K_{p_c a}}$

h   initial pressure rise ratio due to a step change in inlet total

pressure at constant W, W_2, and A; $\dfrac{\left(\dfrac{\partial P_c}{\partial P}\right)_N}{K_{p_c p}}$

G   functional relationship

I   input function

J   polar moment of inertia, (lb-ft)(sec^2)

K   frequency invariant gain

K_{na} speed gain due to area change at constant W, W_2, and P; $\frac{dN}{dA}$, rpm/sq ft

K_{np} speed gain due to inlet total pressure changes at constant W, W_2, and A; $\frac{dN}{dP}$, rpm/lb/sq ft

K_{nw} speed gain due to fuel flow changes at constant A, W_2, and P; $\frac{dN}{dW}$, rpm/lb/hr

K_{nw_2} speed gain due to reheat fuel flow changes at constant W, A, and P; $\frac{dN}{dW_2}$, rpm/lb/hr

$K_{p_c a}$ pressure gain due to area change at constant W, W_2, and P; $\frac{dP_c}{dA} = \frac{dN}{dA}\left(\frac{\partial P_c}{\partial N}\right)_A + \left(\frac{\partial P_c}{\partial A}\right)_N$, lb/sq ft/sq ft

$K_{p_c p}$ pressure gain due to inlet total pressure change at constant W, W_2, and A; $\frac{dP_c}{dP} = \frac{dN}{dP}\left(\frac{\partial P_c}{\partial N}\right)_P + \left(\frac{\partial P_c}{\partial P}\right)_N$

$K_{p_c w}$ pressure gain due to fuel flow changes at constant W_2, A, and P; $\frac{dP_c}{dW} = \frac{dN}{dW}\left(\frac{\partial P_c}{\partial N}\right)_W + \left(\frac{\partial P_c}{\partial W}\right)_N$, lb/sq ft/lb/hr

$K_{p_c w_2}$ pressure gain due to reheat fuel flow changes at constant W, A, and P; $\frac{dP_c}{dW_2} = \frac{dN}{dW_2}\left(\frac{\partial P_c}{\partial N}\right)_{W_2} + \left(\frac{\partial P_c}{\partial W_2}\right)_N$, lb/sq ft/lb/hr

$(K_{nw})_{0.9\ N_r}$ speed gain evaluated at 0.90 N_r, rpm/lb/hr

$(K_{p_c w})_{0.94\ N_r}$ pressure gain evaluated at 0.94 N_r, lb/sq ft/lb/hr

k proportionality factor, lb/sq ft/rpm.

$\mathscr{L}[\ ]$ Laplace transformation

N engine speed, rpm

N_r — rated sea-level engine speed, rpm

O — output function

P — engine inlet total pressure, lb/sq ft

P_c — compressor-discharge total pressure, lb/sq ft

p — number of cycles in time T, cycles

Q — engine torque, ft-lb

s — Laplacian operator

T — total time, sec

t — instantaneous time, sec

W — engine primary fuel flow, lb/hr

W_2 — engine reheat fuel flow, lb/hr

x — input function

Y — variable

y — output function

Δ — incremental change

σ — correction factor, $\left\{ 1 + k \left(\dfrac{\partial N}{\partial P} \right)_{W,A,W_2} \right\}$

τ — engine time constant, sec

τ_1 — engine time constant obtained by AC analysis for engine speed of 0.88 N_r, and amplitude of ±0.01 N_r, sec

τ_f — equivalent fuel system time constant, sec

φ — phase angle, radians

ω — circular frequency, radians/sec

APPENDIX B

DERIVATION OF TRANSFER FUNCTIONS DESCRIBING

ENGINE DYNAMIC BEHAVIOR

Examination of transient data suggests that engine behavior can be described by two general types of transfer functions of the first order (reference 2, ch. 5), the dominant characteristic of which is a speed lag. The simultaneous relationships of pressure, temperature, fuel flow, and air flow lead to quasi-static assumptions, at least for small deviations from the equilibrium point (references 6 and 7). If certain functional relationships are assumed, simple transfer functions result that agree with experimental data. These transfer functions are restricted by the following assumptions:

(1) Engine is considered a lumped constant system.

(2) Linearization about an arbitrary operating point applies.

(3) Conditions of flight speed and altitude are constant.

(4) Only major storage element is rotor inertia, J.

(5) All thermodynamic and flow processes are quasi-static.

(6) All supply sources have zero impedance.

Engine Speed

The experimental speed response of figure 4 to an approximate step disturbance in fuel flow indicates an exponential relationship. If the assumption is made that

$$Q = G(N,W) \qquad (B1)$$

and that linearity applies for small deviations from a steady state or equilibrium point, then

$$\Delta Q = \left(\frac{\partial Q}{\partial W}\right)_N \Delta W + \left(\frac{\partial Q}{\partial N}\right)_W \Delta N \qquad (B2)$$

For a turbojet engine initially in steady state, an incremental increase in fuel flow produces an unbalance torque which accelerates the engine rotor to a new equilibrium speed. Using the relationship

$$\Delta Q = J\Delta \dot{N} \tag{B3}$$

and equating (B3) with (B2) yield

$$J\Delta \dot{N} = \left(\frac{\partial Q}{\partial W}\right)_N \Delta W + \left(\frac{\partial Q}{\partial N}\right)_W \Delta N = J\frac{d}{dt}\Delta N$$

or

$$\Delta N = -\frac{\left(\dfrac{\partial Q}{\partial W}\right)_N}{\left(\dfrac{\partial Q}{\partial N}\right)_W}{1 - \dfrac{J}{\left(\dfrac{\partial Q}{\partial N}\right)_W}\dfrac{d}{dt}}\Delta W \tag{B4}$$

Replacing $\dfrac{d}{dt}$ by the Laplacian operator, for the initial condition of steady state, equation (B4) becomes, in transfer function form (reference 8, ch. 5),

$$\Delta N(s) = \frac{K_{nW}}{1 + \tau s}\Delta W(s) \tag{B5}$$

where the speed gain K_{nW} is $\dfrac{dN}{dW}$ and the engine time constant τ

is $\dfrac{-J}{\left(\dfrac{\partial Q}{\partial N}\right)_W}$

By definition, the transfer function is the ratio of the Laplace transform of the output to the Laplace transform of the input; or from equation (B5)

$$\frac{\mathscr{L}\left[\Delta N\right]}{\mathscr{L}\left[\Delta W\right]} = \frac{\Delta N}{\Delta W}(s) = \frac{K_{nW}}{1 + \tau s} \tag{B6}$$

If the output results from a step input disturbance, then the responses are called indicial responses. The excitation function, or step disturbance, multiplied by the transfer function (equation (B6)) results in a response transform

$$\Delta N(s) = \frac{\Delta W}{s}\frac{K_{nW}}{1 + \tau s}$$

whose inverse transformation is

$$\Delta N(t) = K_{nw}\Delta W \left(1 - e^{-t/\tau}\right) \tag{B7}$$

A theoretical indicial speed response is shown in figure 3, which compares with the experimental indicial response of figure 4. The indicial response function completely defines, as well as the transfer function, the relations of a physical system. If the indicial response is known, it is possible to compute with its help the effect of any arbitrary disturbance which affects the system.

This speed - fuel-flow relationship applies for an idealized engine with only one degree of freedom (constant exhaust nozzle area, zero reheat fuel·flow, and constant inlet total pressure) and subject to the listed restrictions.

Obviously, for changes in only one independent variable, with the others held constant, the following transfer functions apply: for area changes

$$\frac{\Delta N}{\Delta A}(s) = \frac{K_{na}}{1 + \tau s} \tag{B8}$$

for reheat fuel flow changes

$$\frac{\Delta N}{\Delta W_2}(s) = \frac{K_{nW_2}}{1 + \tau s} \tag{B9}$$

and for inlet total pressure changes

$$\frac{\Delta N}{\Delta P}(s) = \frac{K_{np}}{1 + \tau s} \tag{B10}$$

It follows from the linearization assumption that the combined speed response resulting from simultaneous variations of input variables is the superposition of. responses from variations in each·independent variable separately. Thus the addition of equations (B6), (B8), (B9), and (B10) is the combined speed response, or

$$\Delta N(s) = \frac{K_{nw}}{1 + \tau s}\Delta W(s) + \frac{K_{nW_2}}{1 + \tau s}\Delta W_2(s) + \frac{K_{na}}{1 + \tau s}\Delta A(s) + \frac{K_{np}}{1 + \tau s}\Delta P(s) \tag{B11}$$

where the K's are defined in appendix A.

It also follows from the linearization assumption that the engine time constant τ is the same regardless of which independent variable produces acceleration.

The idealized transfer function (equation (B11)) assumes zero impedance sources; that is, there must be no reaction between the engine and the independent variables. However, in turbojet engine test installations, 100 percent regulation of fuel and air supplies is difficult. Fuel flow does not respond instantly to fuel valve setting because of the necessary plumbing; and the variation in combustion chamber pressure during engine acceleration varies the pressure drop across the fuel nozzles and hence varies the fuel flow.

Similarly, air is supplied through large ducting and mass flow is adjusted by throttling. Regulation during acceleration is difficult and engine reactance with air supply is noticeable as indicated by figure 4. If the change in inlet total pressure is assumed proportional to speed,

$$\Delta P = - k \Delta N \qquad (B12)$$

The proportionality constant $(-k)$ is negative if the pressure P decreases for increases in engine speed. For constant exhaust nozzle area and zero reheat fuel flow, equation (B11) becomes

$$\Delta N(s) = \frac{K_{nW}}{1 + \tau s} \Delta W(s) - \frac{K_{np}}{1 + \tau s} k \Delta N(s)$$

or

$$\frac{\Delta N}{\Delta W}(s) = \frac{K_{nW}}{1 + kK_{np}} \left(\frac{1}{1 + \dfrac{\tau}{1 + kK_{np}} s} \right) = \frac{K_{nW}}{\sigma} \left(\frac{1}{1 + \dfrac{\tau}{\sigma} s} \right) \qquad (B13)$$

Thus, the experimental indicial response (fig. 4) includes the variation, during acceleration, of the throttling losses on the air supply. Comparison of equation (B13) with equation (B6) indicates that the time constant $\dfrac{\tau}{\sigma}$ and speed gain $\dfrac{K_{nW}}{\sigma}$ are reduced values because $\sigma = 1 + kK_{np}$ is always greater than one.

The transfer function yields the frequency response function with the substitution $s = i\omega$ (reference 8, ch. 3). If the derivatives are substituted for the K's and $\dfrac{d}{dt}$ for s, the transfer function becomes a linear differential equation.

Compressor-Discharge Total Pressure

The experimental pressure response of figure 4 indicates that there is an initial pressure rise at constant speed due to a fuel flow change, and a subsequent pressure rise at constant fuel flow due to the resultant speed change. If,

$$P_c = G(N,W) \tag{B14}$$

and linearity is assumed for small excursions from the steady state point, then

$$\Delta P_c = \left(\frac{\partial P_c}{\partial W}\right)_N \Delta W + \left(\frac{\partial P_c}{\partial N}\right)_W \Delta N$$

From equation (B4)

$$\Delta P_c = \left(\frac{\partial P_c}{\partial W}\right)_N \Delta W + \frac{\frac{dN}{dW}\left(\frac{\partial P_c}{\partial N}\right)_W}{1 + \tau \frac{d}{dt}} \Delta W = \frac{\frac{dN}{dW}\left(\frac{\partial P_c}{\partial N}\right)_W + \left(\frac{\partial P_c}{\partial W}\right)_N + \left(\frac{\partial P_c}{\partial W}\right)_N \tau \frac{d}{dt}}{1 + \tau \frac{d}{dt}} \Delta W$$

$$= K_{p_c W} \frac{1 + d\tau \frac{d}{dt}}{1 + \tau \frac{d}{dt}} \Delta W \tag{B15}$$

where $K_{p_c W} = \frac{dN}{dW}\left(\frac{\partial P_c}{\partial N}\right)_W + \left(\frac{\partial P_c}{\partial W}\right)_N = \frac{dP_c}{dW} = $ pressure gain

and $d = \dfrac{\left(\dfrac{\partial P_c}{\partial W}\right)_N}{K_{p_c W}} = $ initial pressure rise ratio. In transfer function

form, equation (B15) becomes

$$\frac{\Delta P_c}{\Delta W}(s) = \frac{1 + d\tau s}{1 + \tau s} K_{p_c W} \tag{B16}$$

The response transform to a unit step excitation function is

$$\Delta P_c(s) = \frac{1 + d\tau s}{1 + \tau s} \frac{1}{s} K_{p_c W} \Delta W$$

whose inverse transformation is

$$\Delta P_c(t) = K_{p_c W}\Delta W \left[1 - (1 - d)e^{-t/\tau}\right] \tag{B18}$$

A theoretical indicial pressure response which compares with the experimental indicial response of figure 4 is shown in figure 3.

Again, as with the combined speed response, it follows from the linearization assumption that the pressure response resulting from simultaneous variations of input variables is

$$\Delta P_c(s) = K_{p_c W}\left\{\frac{1 + d\tau s}{1 + \tau s}\right\}\Delta W(s) + K_{p_c W_2}\left\{\frac{1 + f\tau s}{1 + \tau s}\right\}\Delta W_2(s) +$$

$$K_{p_c a}\left\{\frac{1 + g\tau s}{1 + \tau s}\right\}\Delta A(s) + K_{p_c P}\left\{\frac{1 + h\tau s}{1 + \tau s}\right\}\Delta P(s) \tag{B19}$$

The values of the K's and d, f, g, and h are defined in appendix A.

If, again, the change in inlet total pressure is assumed to be proportional to the speed change,

$$\Delta P_c = \left\{\left[\left(\frac{\partial P_c}{\partial N}\right)_{W,P} - k\left(\frac{\partial P_c}{\partial P}\right)_{N,W}\right]\Delta N + \left(\frac{\partial P_c}{\partial W}\right)_{N,P}\Delta W\right.$$

or, with the use of equation (B13),

$$\frac{\Delta P_c}{\Delta W}(s) = \left\{\left[\left(\frac{\partial P_c}{\partial N}\right)_{W,P} - k\left(\frac{\partial P_c}{\partial P}\right)_{N,W}\right]\frac{K_{nw}}{\sigma}\left(\frac{1}{1 + \frac{\tau}{\sigma}s}\right) + \left(\frac{\partial P_c}{\partial W}\right)_{N,P}\right.$$

$$= \frac{\frac{K_{nw}}{\sigma}\left[\left(\frac{\partial P_c}{\partial N}\right)_{W,P} - k\left(\frac{\partial P_c}{\partial P}\right)_{N,W}\right] + \left(\frac{\partial P_c}{\partial W}\right)_{N,P} + \left(\frac{\partial P_c}{\partial W}\right)_{N,P}\frac{\tau}{\sigma}s}{1 + \frac{\tau}{\sigma}s} \tag{B20}$$

where the experimental pressure response now includes the variation of the throttling losses on the air supply, or

$$K'_{nw} = \frac{K_{nw}}{\sigma}\left[\left(\frac{\partial P_c}{\partial N}\right)_{W,P} - k\left(\frac{\partial P_c}{\partial P}\right)_{N,W}\right] + \left(\frac{\partial P_c}{\partial W}\right)_{N,P}$$

In comparison with equation (B16), the initial rise $\left(\dfrac{\partial P_c}{\partial W}\right)_{N,P}$ remains the same because it is the pressure rise due to fuel flow changes and it occurs initially at constant speed. The additional pressure rise, however, is $\dfrac{K_{nw}}{\sigma}\left[\left(\dfrac{\partial P_c}{\partial N}\right)_P - k\left(\dfrac{\partial P_c}{\partial P}\right)_N\right]_W$, which compares with $K_{nw}\left(\dfrac{\partial P_c}{\partial N}\right)_W$ of equation (B16). This additional pressure rise, at constant fuel flow, due to speed change is a reduced value. Consequently the initial pressure rise ratio

$$d = \frac{\left(\dfrac{\partial P_c}{\partial N}\right)_N}{K'_{nw}}$$

is an increased value.

The observed responses of any pressure, temperature, or thrust are similar to the response of compressor-discharge total pressure. Thus, the development of the respective transfer functions is similar to the foregoing development.

APPENDIX C

FOURIER ANALYSIS OF TRANSIENT DATA

It is possible to transform from the time domain to the frequency domain if an arbitrary input and corresponding output are known. If the input and output are related by a transfer function, then

$$KG(s) = \frac{\mathscr{L}[y(t)]}{\mathscr{L}[x(t)]} = \frac{\mathscr{L}[output]}{\mathscr{L}[input]} \tag{C1}$$

For a system initially at rest,

$$\mathscr{L}[\dot{y}(t)] = s\mathscr{L}[y(t)]$$

so that in this case

$$KG(s) = \frac{s\mathscr{L}[\dot{y}(t)]}{s\mathscr{L}[\dot{x}(t)]} = \frac{\int_0^\infty \dot{y}(t)e^{-st}\ dt}{\int_0^\infty \dot{x}(t)e^{-st}\ dt} \tag{C2}$$

where the numerator and denominator are unilateral Laplace transforms of $\dot{y}(t)$ and $\dot{x}(t)$.

Because e^{-st} is continuous and $y(t)$ is of bounded variation in $(0,\infty)$, the Stieltjes integral of e^{-st} with respect to $y(t)$ from 0 to ∞ exists (reference 10, p. 7).

If both the numerator and denominator of equation (C2) converge, they define a function of s called the Laplace-Stieltjes transforms of $y(t)$ and $x(t)$, respectively (for example, reference 10, ch. 2).

$$G(s) = \int_0^\infty e^{-st}\ d[y(t)] \tag{C3}$$

However, if

$$G(s) = \int_0^\infty e^{-st}\ y(t)dt$$

then $G(s)$ is the Laplace transform of $y(t)$.

If $\dot{y}(t)$ and $\dot{x}(t)$ exist for $t > 0$ and approach zero sufficiently fast such that $y(t)$ and $x(t)$ are approximately constant for $t > T$, then equation (C1) becomes

$$KG(s) = \frac{\displaystyle\int_0^T e^{-st}\,\dot{y}(t)dt}{\displaystyle\int_0^T e^{-st}\,\dot{x}(t)dt} \tag{C4}$$

By the transformation $s = i\omega$, equation (C4) can be written as a Fourier-Stieltjes transform (reference 10, p. 252); and the frequency response function can now be expressed as (reference 11)

$$KG(i\omega) = \frac{\displaystyle\int_0^T e^{-i\omega t}\dot{y}(t)dt}{\displaystyle\int_0^T e^{-i\omega t}\dot{x}(t)dt}$$

$$= \frac{\displaystyle\int_0^T \dot{y}(t)\cos \omega t\, dt - i\int_0^T \dot{y}(t)\sin \omega t\, dt}{\displaystyle\int_0^T \dot{x}(t)\cos \omega t\, dt - i\int_0^T \dot{x}(t)\sin \omega t\, dt} \tag{C5}$$

Thus there are two types of integrals to be evaluated

$$KG(i\omega) = \frac{\text{Re}\big[y(t)\big] - i\,\text{Im}\big[y(t)\big]}{\text{Re}\big[x(t)\big] - i\,\text{Im}\big[x(t)\big]} \tag{C6}$$

Consider

$$\text{Re}\big[y\big] = \int_0^T \dot{y}(t)\,\cos \omega t\, dt = \int_0^T \cos \omega t\, dy$$

Let

$$Y = y_f - y$$

where y_f is the final value, then

$$dY = 0 - dy$$

At $t = 0$,

$$y = y_0$$

$$Y = y_f - y_0 = Y_0$$

at $t = T,$

$$y = y_f$$

$$Y = y_f - y_f = 0$$

Thus

$$\text{Re}\left[\overline{y}\right] = -\int_T^0 \cos \omega t \; dY = \int_0^T \cos \omega t \; dY$$

Integration by parts gives

$$\text{Re}\left[\overline{y}\right] = Y \cos \omega t \Big|_0^T + \omega \int_T^0 Y \sin \omega t \; dt$$

$$= Y_0 - \omega \int_0^T Y \sin \omega t \; dt \qquad\qquad (C7)$$

Similarly,

$$\text{Im}\left[\overline{y}\right] = \int_0^T \sin \omega t \; dY$$

$$\text{Im}\left[\overline{y}\right] = Y \sin \omega t \Big|_0^T - \omega \int_T^0 Y \cos \omega t \; dt = 0 + \omega \int_0^T Y \cos \omega t \; dt$$

$$(C8)$$

Let T = total transient time and p = number of cycles in time T.
The domain $0 \leqslant t \leqslant T$ is divided into 120 equal intervals; and the
integration is done by using a seven-point numerical integration
scheme (reference 12, pt. II, p. 233), in conjunction with a digital
computor,

$$\int_0^6 y \; dt = \frac{1}{140}\left[41y_0 + 216y_1 + 27y_2 + 272y_3 + 27y_4 + 216y_5 + 41y_6\right]$$

$$(C9)$$

then

$$\omega = 2\pi \; \frac{\text{radians}}{\text{cycle}} \times \frac{p \text{ cycles}}{120 \text{ ordinates}} \times \frac{120 \text{ ordinates}}{T \text{ sec}} = \frac{2\pi p}{T} \; \frac{\text{radians}}{\text{sec}}$$

and

$$\mathrm{Re}[y] = Y_0 - \frac{2\pi p}{T} \frac{T}{120} \sum_{t=0}^{120} A_t \sin \frac{\pi p}{60} t$$

or

$$\mathrm{Re}[y] = Y_0 - \frac{\pi p}{60} \sum_{t=0}^{120} A_t \sin \frac{\pi p}{60} t$$

and

$$\mathrm{Im}[y] = \frac{\pi p}{60} \sum_{t=0}^{120} A_t \cos \frac{\pi p}{60} t$$

where

$$A_0 = \frac{41}{140} \quad Y_0 = \frac{41}{140} (y_f - y_0)$$

$$A_1 = \frac{216}{140} \quad Y_1 = \frac{216}{140} (y_f - y_1)$$

$$A_2 = \frac{27}{140} \quad Y_2 = \frac{27}{140} (y_f - y_2)$$

. . .

Thus the frequency response function can be readily evaluated for each frequency ω.

$$KG(i\omega) = \frac{A(\omega) - iB(\omega)}{C(\omega) - iD(\omega)} \tag{C10}$$

The amplitude and phase are determined in well-known fashion as

$$K|G(i\omega)| = \sqrt{\frac{A^2 + B^2}{C^2 + D^2}} \tag{C11}$$

$$\varphi = \tan^{-1} \frac{AD - BC}{AC + BD} \tag{C12}$$

REFERENCES

1. v. Kármán, Theodore, and Biot, Maurice A.: Mathematical Methods in Engineering. McGraw-Hill Book Co., Inc., 1940.

2. Brown, Gordon S., and Campbell, Donald P.: Principles of Servo-mechanisms. John Wiley & Sons, Inc., 1948.

3. Anon.: Theory of Servomechanisms, Hubert M. James, Nathaniel B. Nichols, and Ralph S. Phillips, eds. McGraw-Hill Book Co., Inc., 1947.

4. Johnson, Walter C.: Transmission Lines and Networks. McGraw-Hill Book Co., Inc., 1950.

5. Delio, Gene J., Schwent, Glennon V., and Cesaro, Richard S.: Transient Behavior of Lumped-Constant Systems for Sensing Gas Pressures. NACA TN 1988, 1949.

6. Otto, Edward W., and Taylor, Burt L., III: Dynamics of a Turbojet Engine Considered as a Quasi-Static System. NACA Rep. 1011, 1951. (Formerly NACA TN 2091.)

7. Feder, Melvin S., and Hood, Richard: Analysis for Control Application of Dynamic Characteristics of Turbojet Engine with Tail-Pipe Burning. NACA TN 2183, 1950.

8. Gardner, Murray F., and Barnes, John L.: Transients in Linear Systems. Vol. I. John Wiley & Sons, Inc., 1942.

9. Bode, Hendrick W.: Network Analysis and Feedback Amplifier Design. D. Van Nostrand Co., Inc., 1945.

10. Widder, David Vernon: The Laplace Transform. Princeton University Press, 1946.

11. LaVerne, Melvin E., and Boksenbom, Aaron S.: Frequency Response of Linear Systems from Transient Data. NACA Rep. 977, 1950. (Formerly NACA TN 1935.)

12. Lipka, Joseph: Graphical and Mechanical Computations. Pt. II. Experimental Data. John Wiley & Sons, Inc., 1918.

TABLE I - VARIATION OF ENGINE DYNAMIC

CHARACTERISTICS WITH MAGNITUDE

OF DISTURBANCE

[Average operating point = 0.94 N_r]

Magnitude of disturbance (percent N_r)	Engine time constant τ / τ_1	Initial pressure rise ratio, d
1	0.78	0.80
2	.74	.80
4	.68	.75
8	.61	.71

TABLE II - VARIATION OF ENGINE DYNAMIC

CHARACTERISTICS AS DETERMINED

BY AC ANALYSIS

[Amplitude of disturbance at zero frequency = ±0.01 N_r]

Operating point (percent N_r)	Engine time constant τ / τ_1	Initial pressure rise ratio, d
98	0.67	0.81
94	.87	.70
88	1.00	.54

TABLE III - VARIATION OF ENGINE DYNAMIC

CHARACTERISTICS WITH MAGNITUDE

OF DISTURBANCE AS DETERMINED

BY FREQUENCY RESPONSE

[Operating point = 0.94 N_r]

Amplitude of disturbance (percent N_r)	Engine time constant τ/τ_1	Initial pressure rise ratio, d
±1	0.87	0.70
±2	.86	.72
±3.5	.72	.78
±6	.67	.80

TABLE IV - COMPARISON OF ENGINE DYNAMIC

CHARACTERISTICS OBTAINED BY TWO

METHODS OF ANALYSIS FOR

0.01 N_r DISTURBANCES

Operating point (percent N_r)	Transient analysis		AC analysis	
	Engine time constant τ/τ_1	Initial rise ratio d	Engine time constant τ/τ_1	Initial rise ratio d
98	0.61	0.92	0.67	0.81
94	.78	.80	.87	.70
88	.98	.67	1.00	.54

TABLE V - COMPARISON OF ENGINE DYNAMIC CHARACTERISTICS

OBTAINED BY TWO METHODS OF ANALYSIS FOR VARYING

MAGNITUDES OF DISTURBANCES

[Average operating point = 0.94 N_r]

Transient analysis			AC analysis		
Magnitude of disturbance (percent N_r)	Engine time constant τ/τ_1	Initial rise ratio d	Amplitude of disturbance (percent N_r)	Engine time constant τ/τ_1	Initial rise ratio d
1	0.78	0.80	±1	0.87	0.70
2	.74	.80	±2	.86	.72
4	.68	.75	±3.5	.72	.78
8	.61	.71	±6	.67	.80

TABLE VI - COMPARISON OF ENGINE DYNAMIC CHARACTERISTICS

OBTAINED BY THREE METHODS OF ANALYSIS

[Average operating point = 0.94 N_r;

approximate magnitude of disturbance = 0.08 N_r]

Method of analysis	Engine time constant τ/τ_1	Initial rise ratio d
Transient	0.61	0.71
Fourier	.67	.80
Frequency response	.67	.80
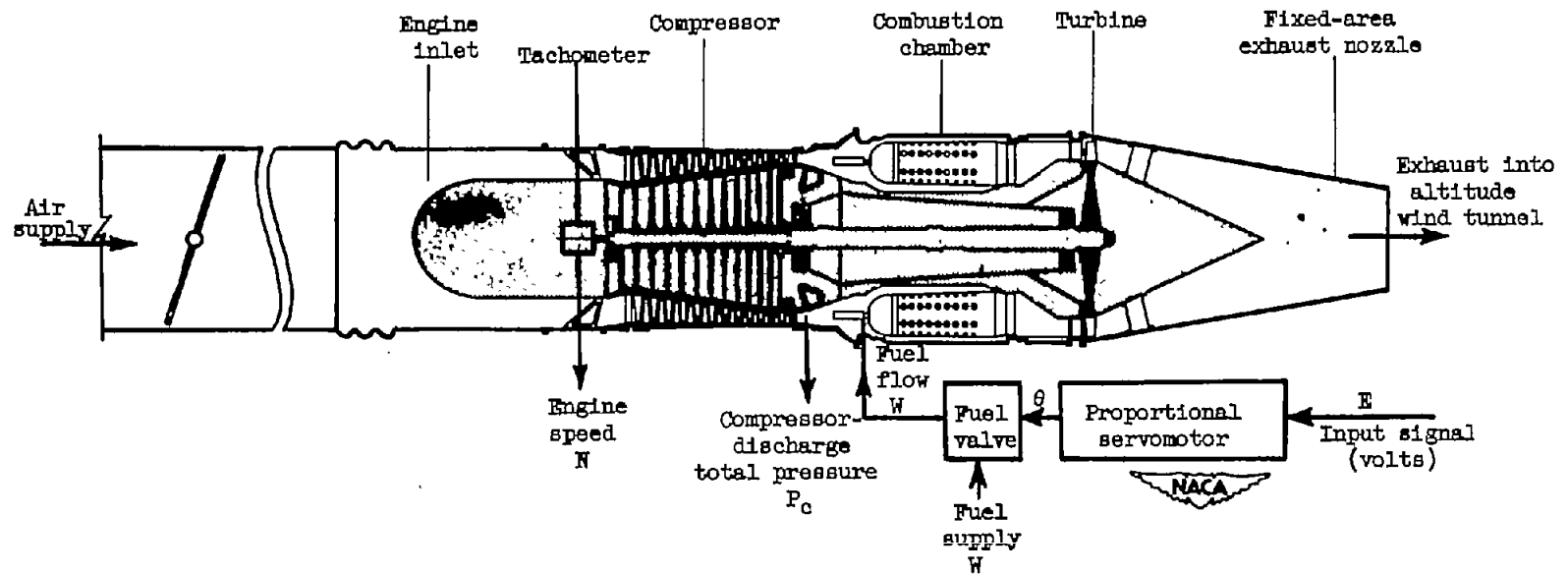
Figure 1. - Turbojet engine installation illustrating supply sources and control, and location of sensing elements.

Speed sensor

$K = 1.0 \frac{mv}{rpm}$

Filter

"Constant k" filter

$\omega_c = 50 \frac{rad}{sec}$

Balance

Amplifier and recorder

$K = 1.0 \frac{mm}{mv}$

DC to 100 cps
(essentially flat)

Maximum pen sensitivity

$1.0 \frac{rpm}{mm}$

N(rpm)   E   E   E   E

(a) Engine speed.

Pressure sensor

Pneumatic system

$\frac{1}{\frac{s^2}{2500} + \frac{1.2}{50} S + 1}$

Transducer

$K = 25 \frac{\mu in.}{in.} \frac{1}{in. Hg}$

$\varepsilon \left(\frac{\mu in.}{in.} \right)$

Strain amplifier and recorder

$K = \frac{0.4 \text{ mm pen displacement}}{\mu in./in. \text{ strain}}$

DC to 100 cps
(essentially flat)

P(in. Hg)

$0.1 \frac{in. Hg}{mm}$
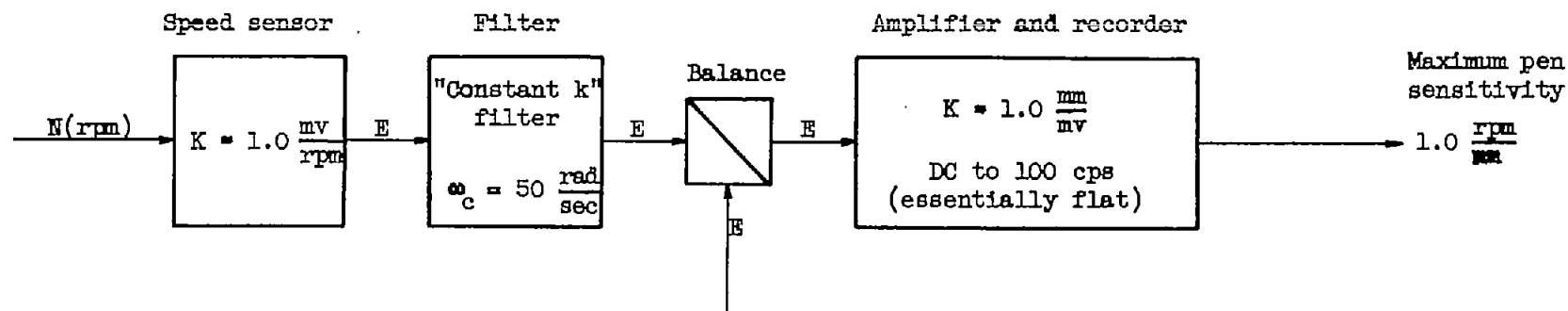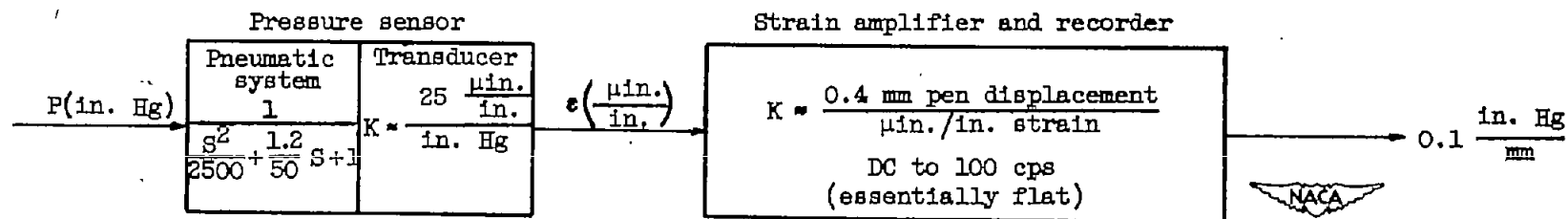
(b) Pressure.

Figure 2. - Dynamic characteristics of two basic sensing systems for recording transient engine behavior.
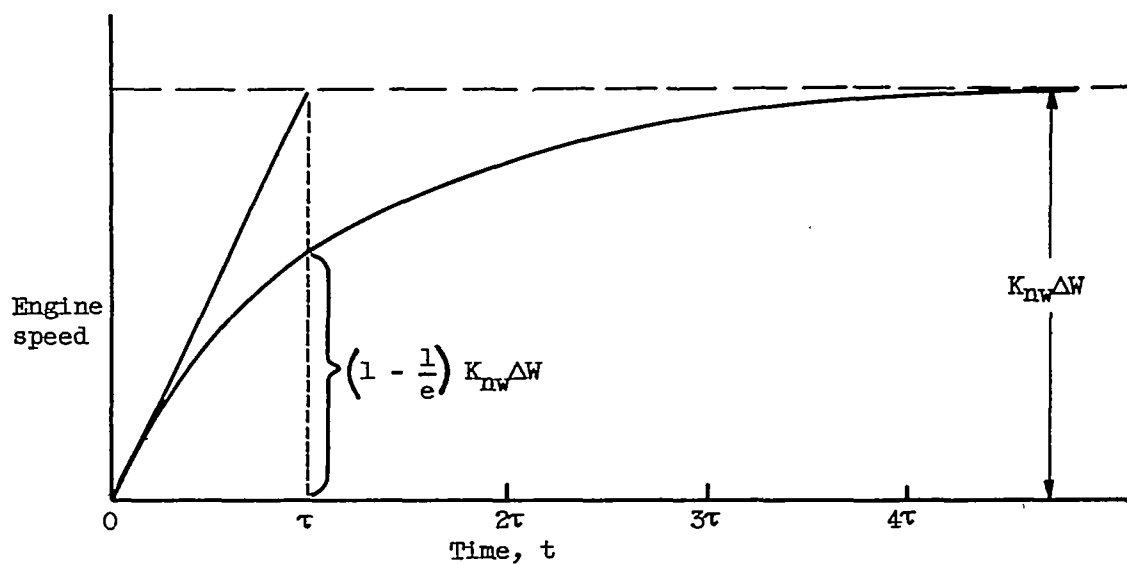
(a) Engine speed.
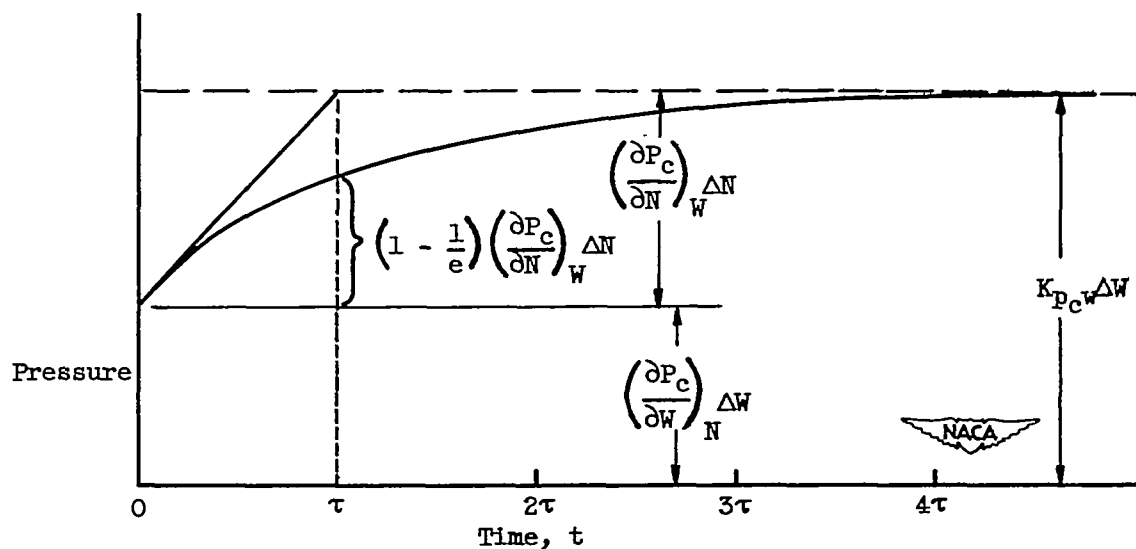
(b) Compressor-discharge total pressure.

Figure 3. - Theoretical indicial responses of pressure and
engine speed to fuel flow.
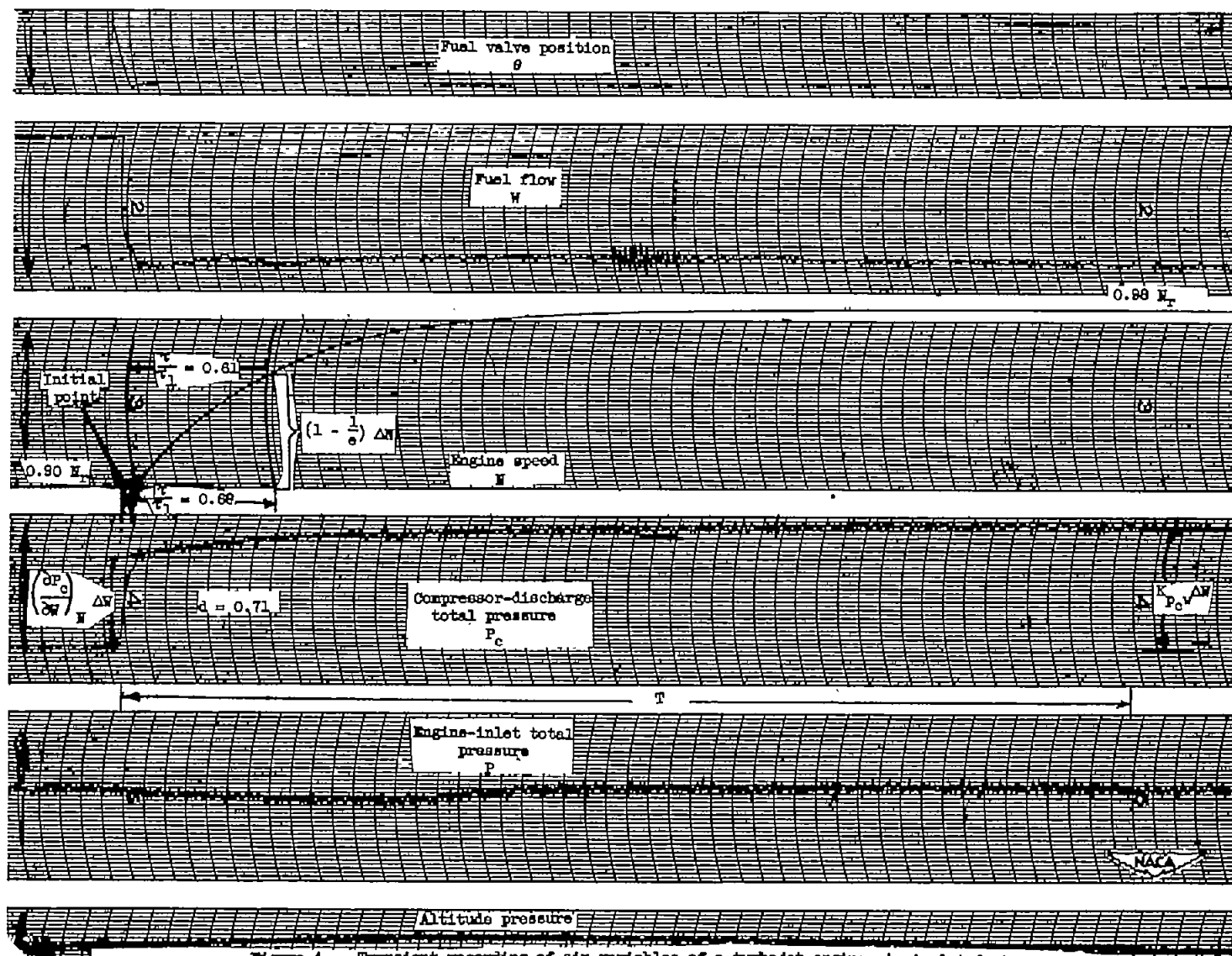
Figure 4. - Transient recording of six variables of a turbojet engine at simulated altitude of 15,000 feet and simulated flight Mach number of 0.22.

Imaginary

— Direct calculation
O Fourier analysis approxi-
   mation by digital com-
   puter for 24 discrete
   frequencies

ω_{24}

$\dfrac{1 + 8.8s}{1 + 8s}$

1.0

-.3 -.2 0 .1 .2 .3 .4 .5 .6 .7 .8 .9 1.1 Real

ω

Approximated
245°

Calculated
207°

-.1

Calculated and
approximated

$\phi = \left(-0.4\omega_1 - \tan^{-1} 4\omega_1\right)$

ω_2 ω_1

ω_3

ω_4

ω_5

-.2

ω_6

-.3

ω_7

-.4

$\dfrac{e^{-0.4s}}{1 + 4s}$

ω_8

-.5

$\leftarrow\omega$

ω_9

-.6

NACA
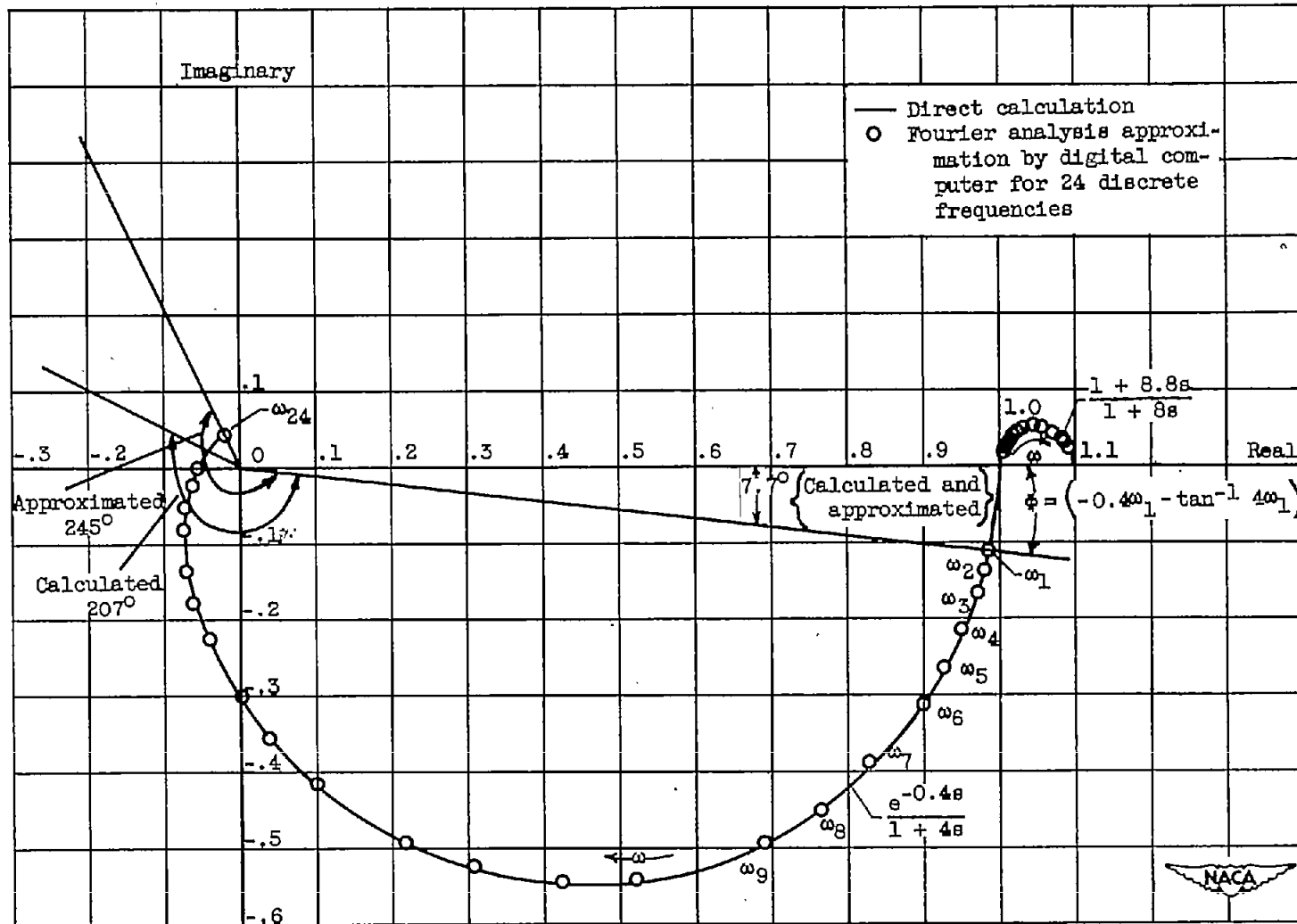
Figure 5. - Transfer loci of $\left(\dfrac{e^{-0.4s}}{1 + 4s}\right)$ and $\left(\dfrac{1 + 8.8s}{1 + 8s}\right)$ to an assumed step; obtained by direct calculation and by Fourier analysis performed by digital computer.
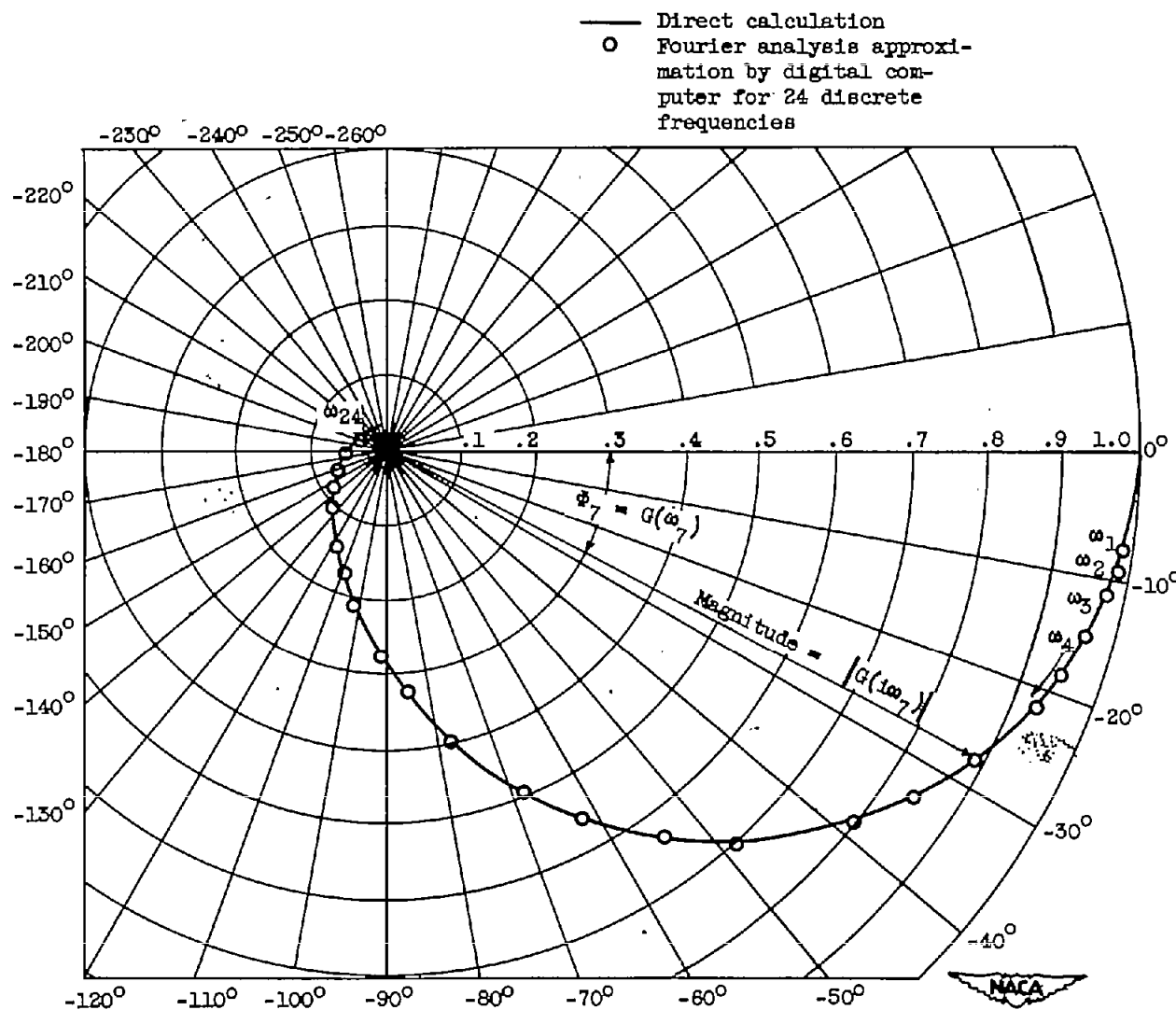
Figure 6. – Transfer function $G(s) = \dfrac{e^{-0.4s}(1 + 8.8s)}{(1 + 4s)(1 + 8s)}$ determined from figure 5.

(a) $G(s) = \dfrac{1}{1 + s}$
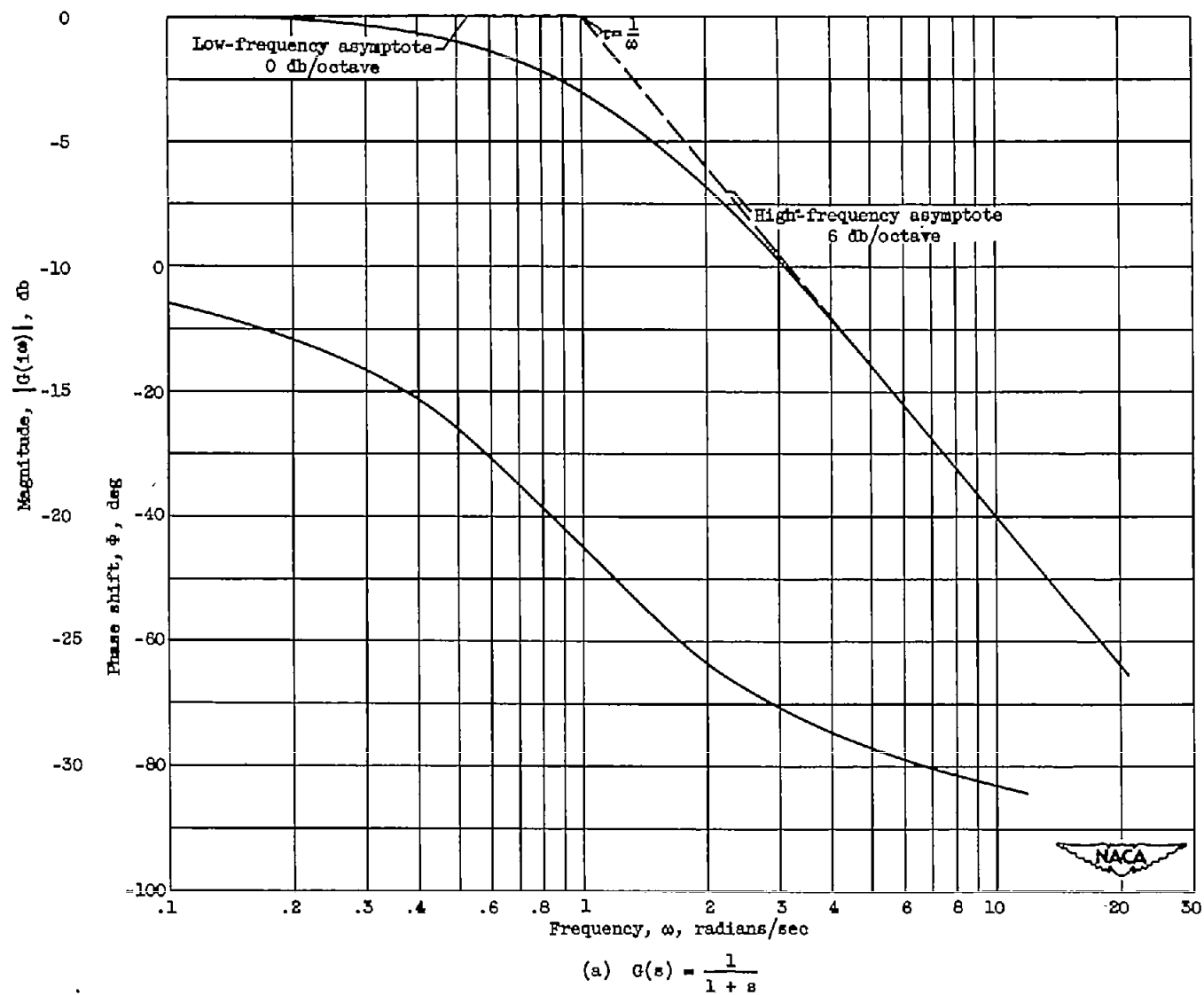
Figure 7. - Frequency spectra of a first-order dynamic system.

$$(b) \quad G(s) = \frac{1 + 0.5s}{1 + s}$$
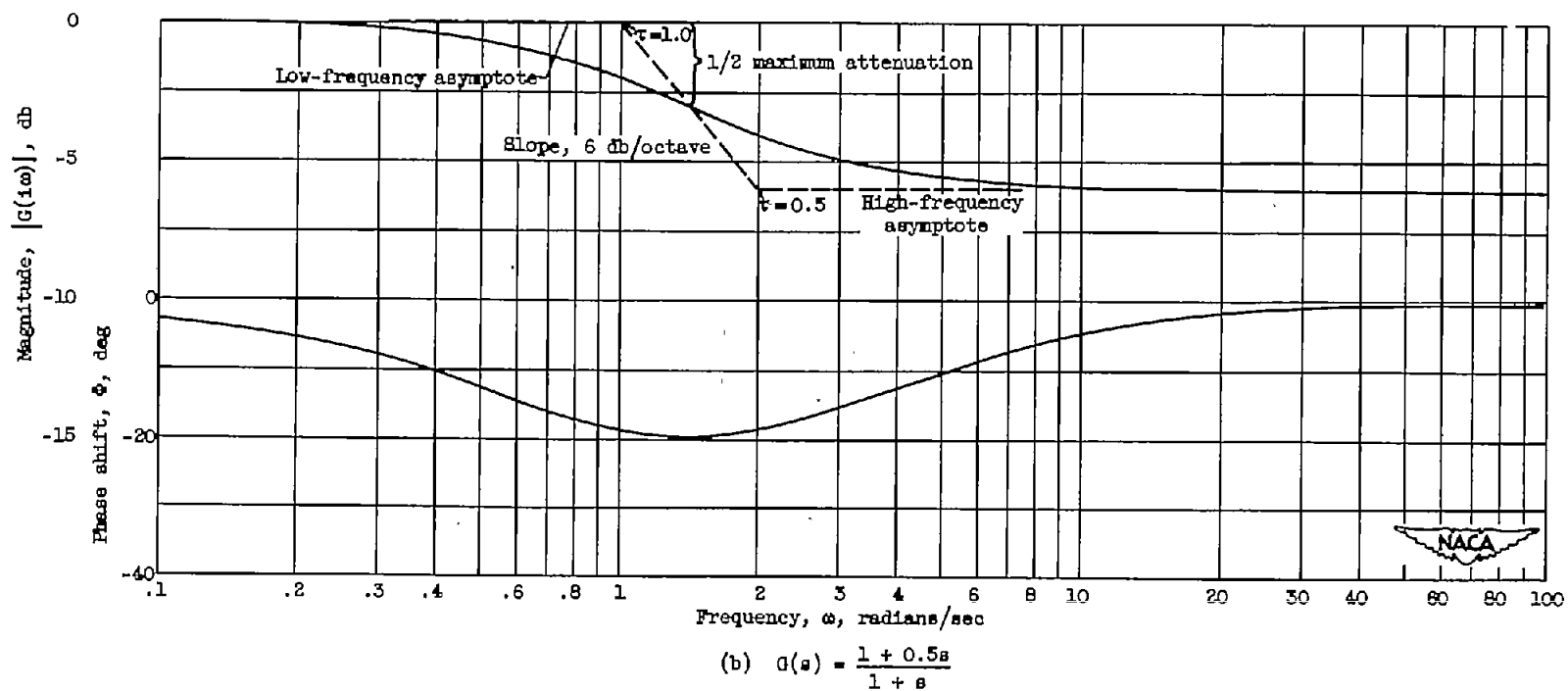
Figure 7. - Concluded. Frequency spectra of a first-order dynamic system.
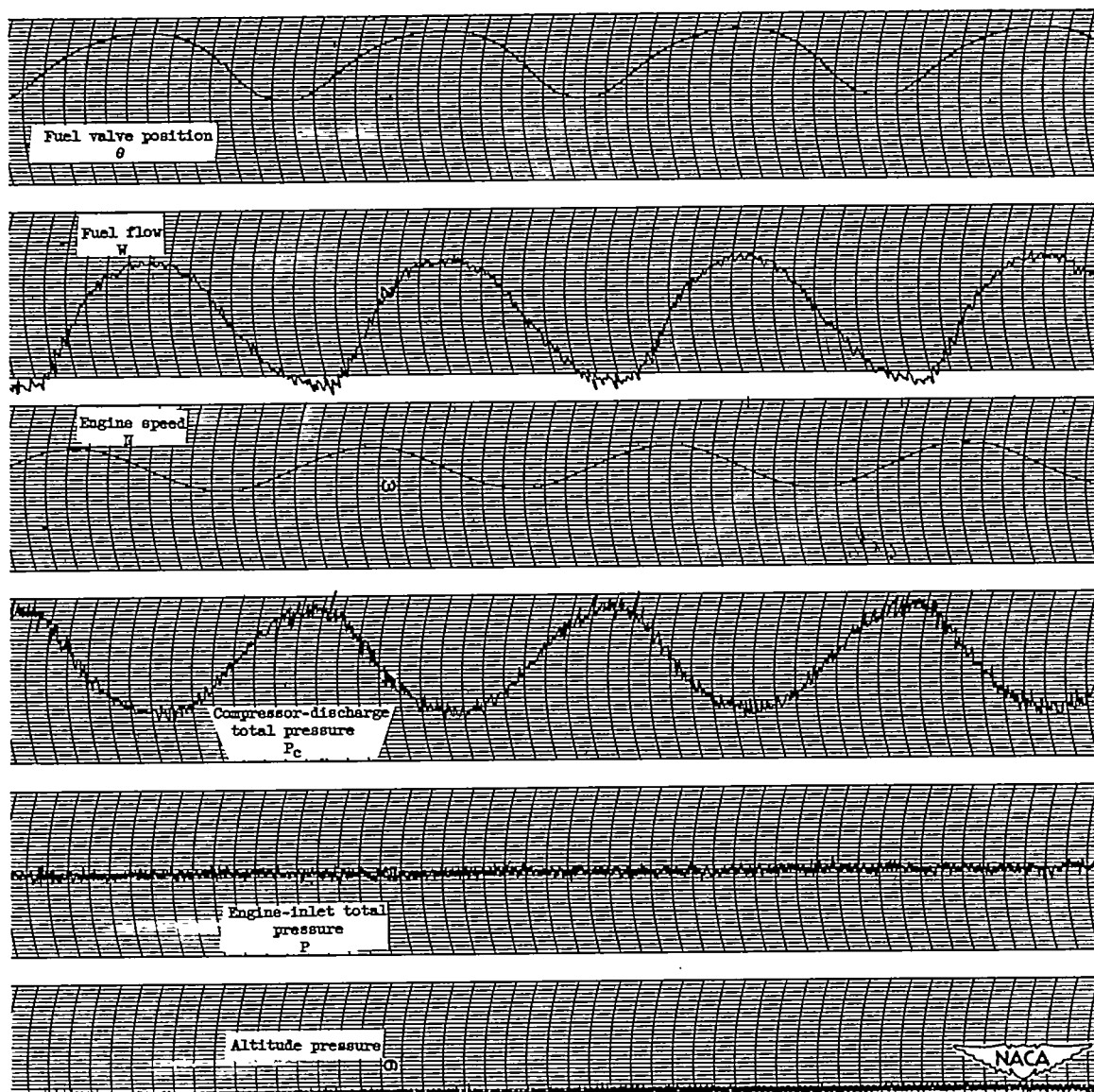
Figure 8. - Typical transient data obtained by sinusoidal variation of fuel valve position of turbojet engine at simulated altitude of 15,000 feet and simulated flight Mach number of 0.22.

Figure 9. - Variation of several engine gains with speed for a turbojet engine operating at simulated altitude of 15,000 feet and simulated flight Mach number of 0.22.
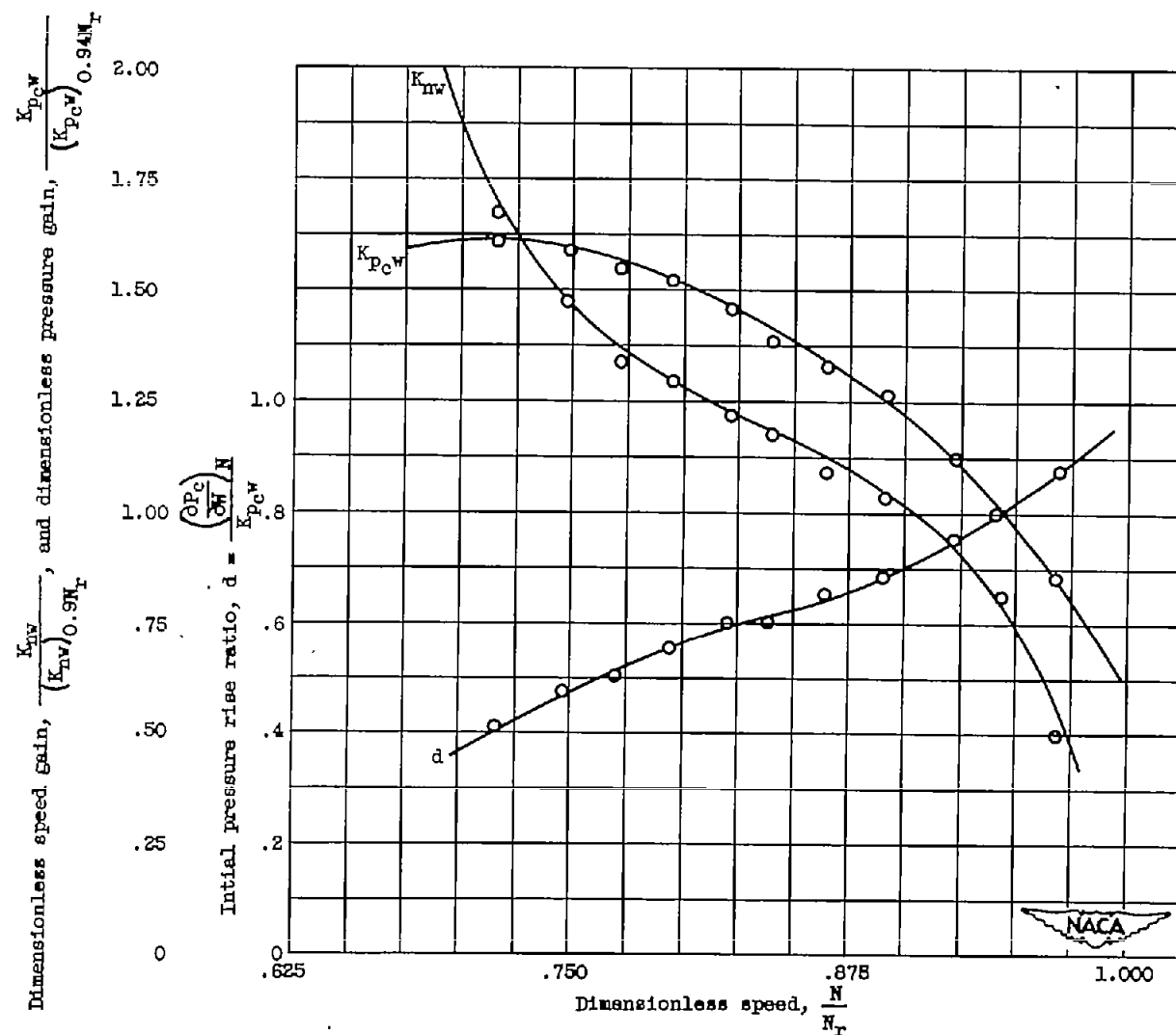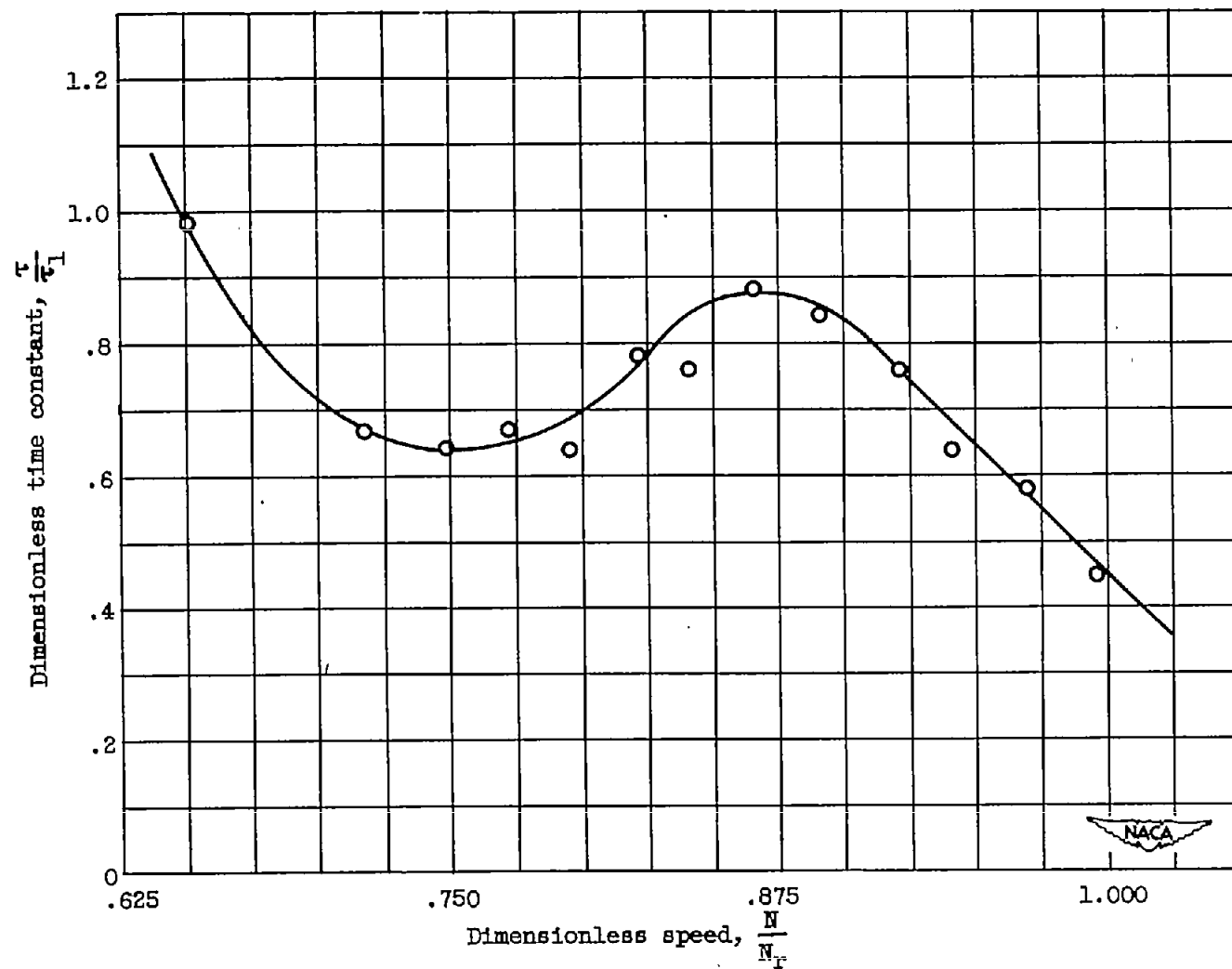
Figure 10. - Variation of engine time constant with speed for a turbojet engine operating at simulated altitude of 15,000 feet and simulated flight Mach number of 0.22.
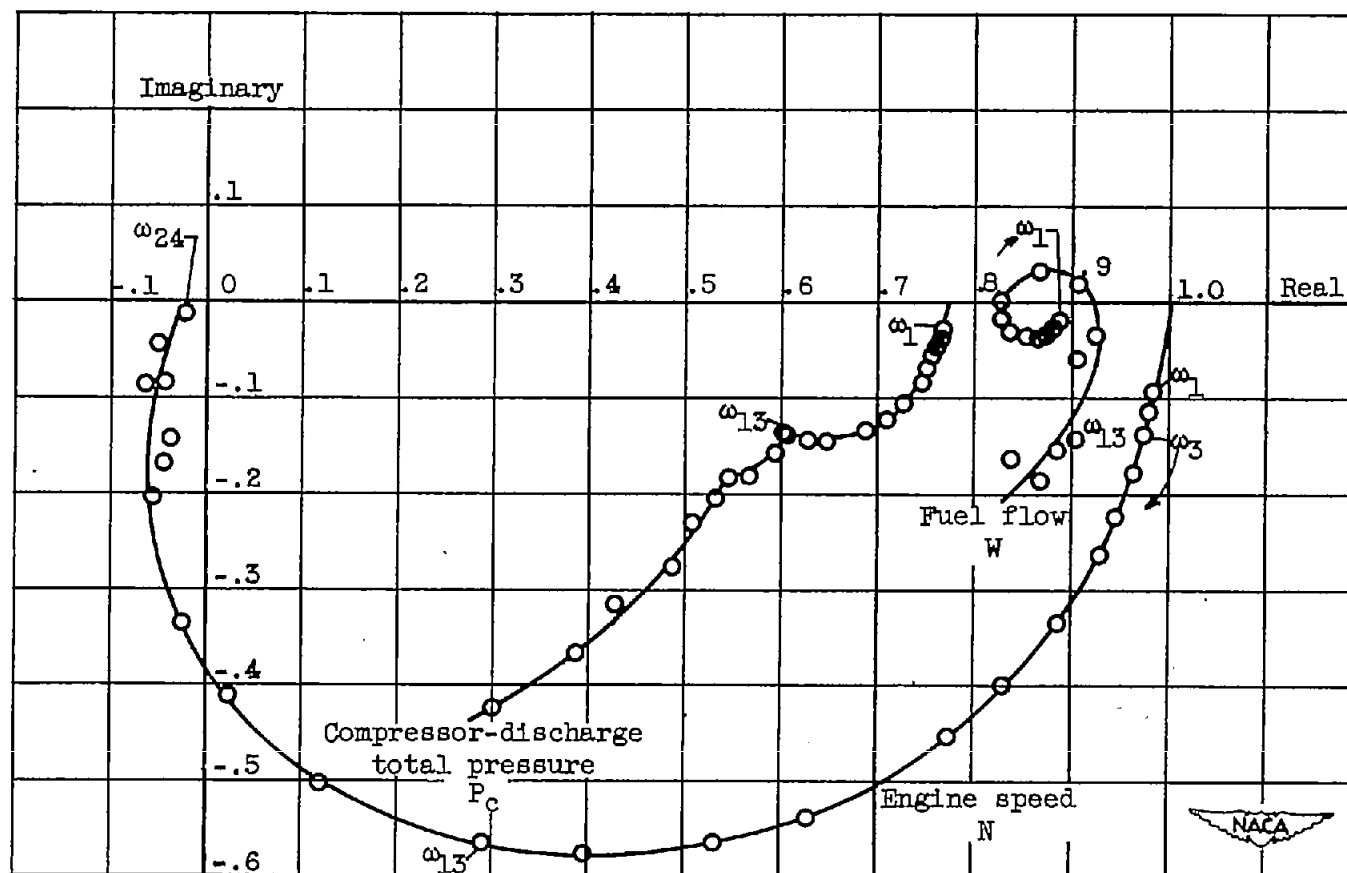
Figure 11. - Fourier analysis of transient responses of figure 4, of engine speed, fuel flow, and compressor-discharge total pressure, to assumed step disturbance.
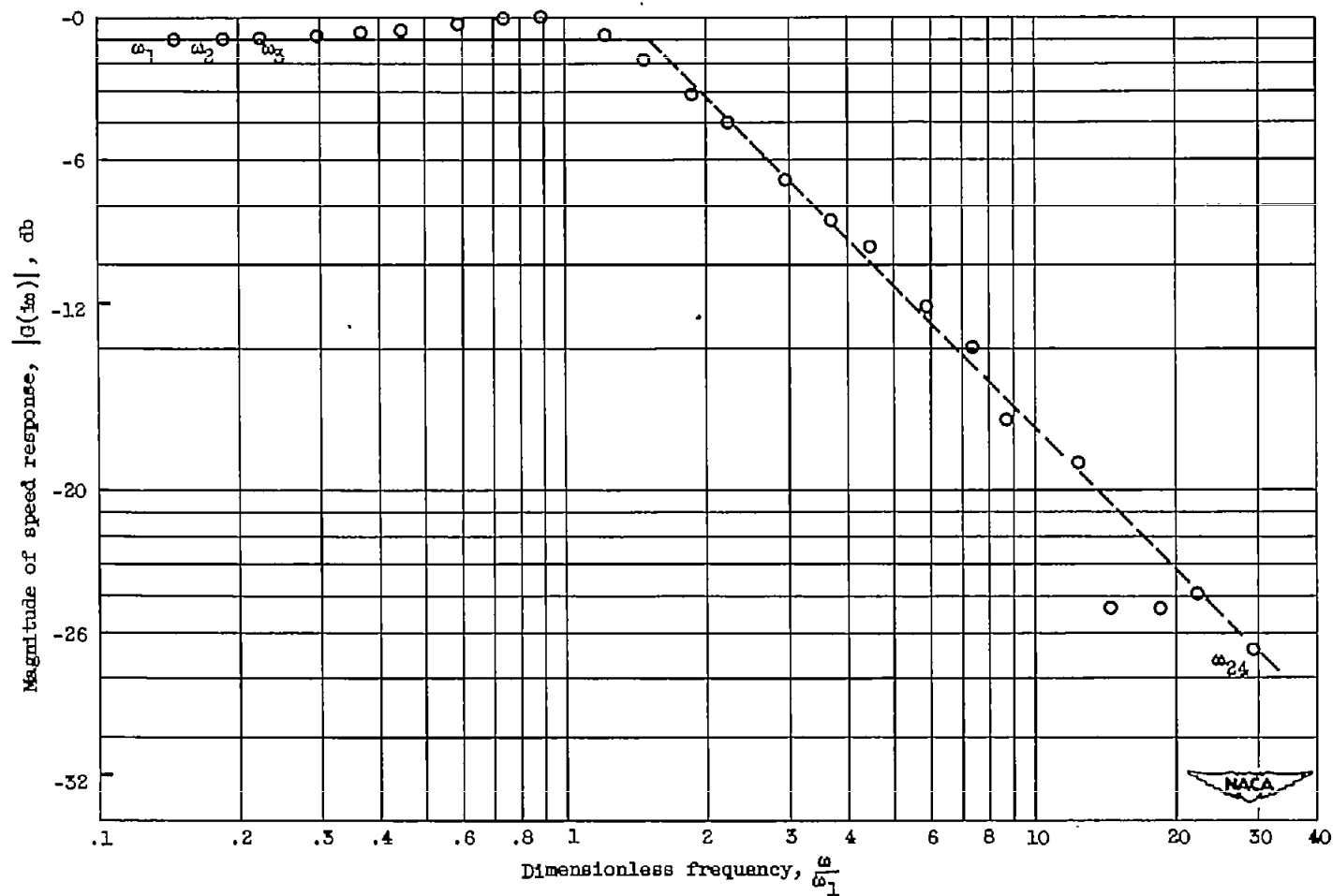
(a) Amplitude ratio.

Figure 12. - Frequency spectrum of engine speed response to fuel flow, obtained by Fourier analysis of transient responses of figure 4, of turbojet engine for simulated altitude of 15,000 feet and simulated flight Mach number of 0.22.
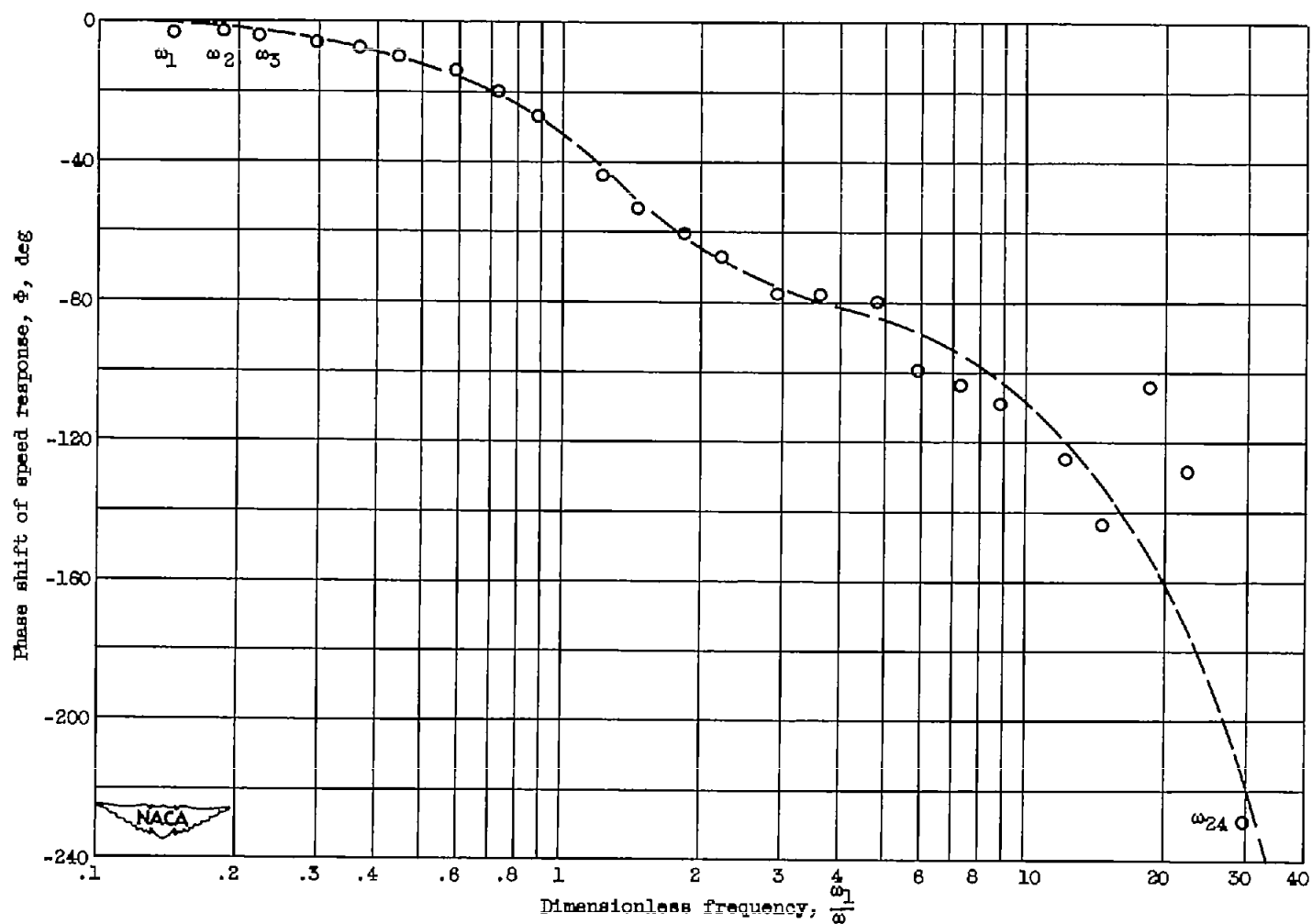
(b) Phase shift.

Figure 12. - Concluded. Frequency spectrum of engine speed response to fuel flow, obtained by Fourier analysis of transient responses of figure 4, of turbojet engine for simulated altitude of 15,000 feet and simulated flight Mach number of 0.22.
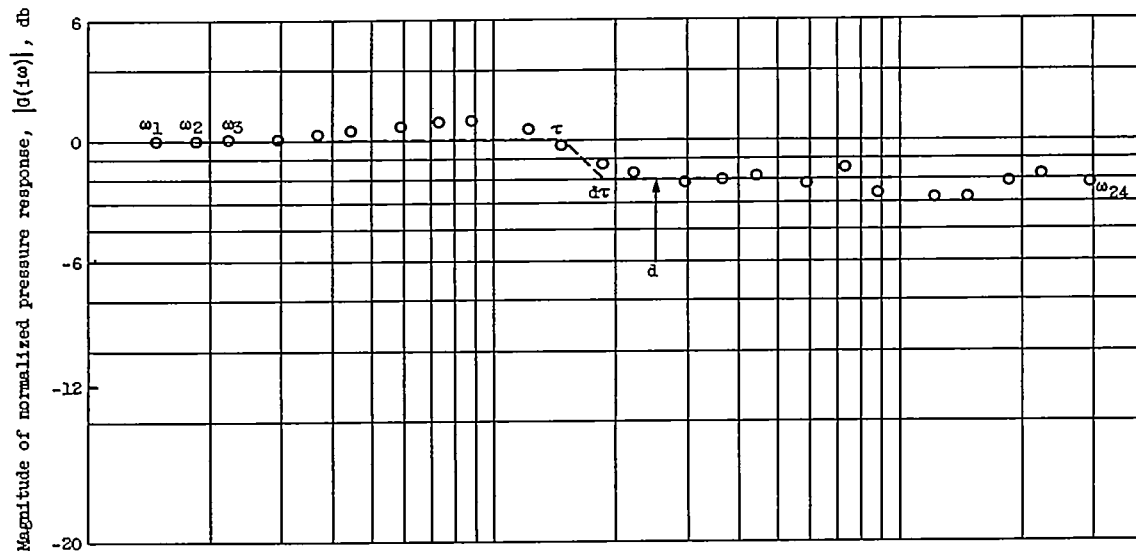
(a) Amplitude ratio.
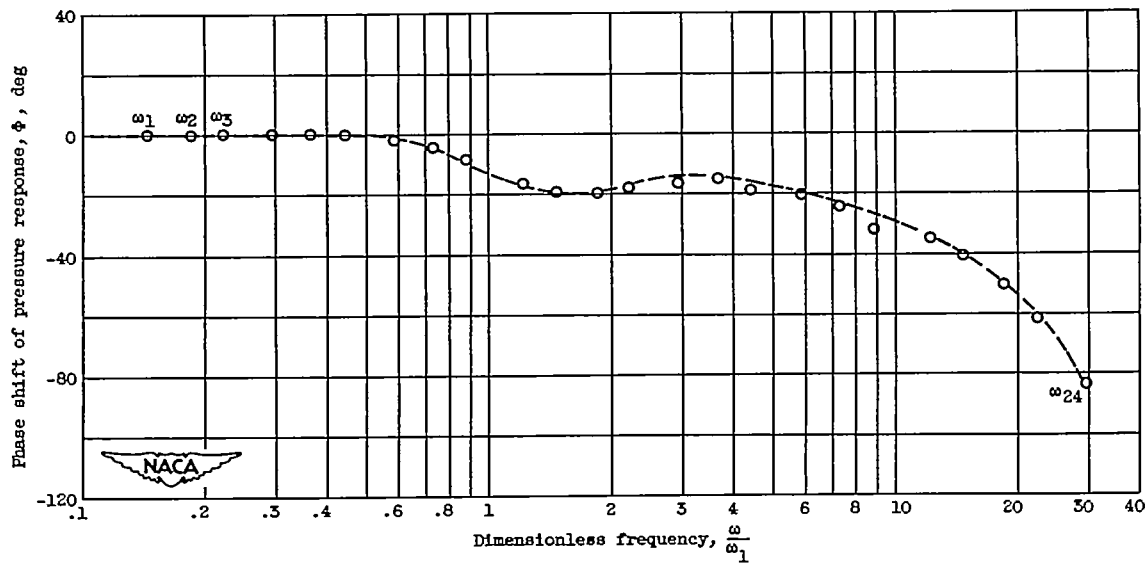
(b) Phase shift.

Figure 13. - Frequency spectrum of compressor-discharge total pressure response to fuel flow, obtained
by Fourier analysis of transient responses of figure 4, of turbojet engine at simulated altitude
of 15,000 feet and simulated flight Mach number of 0.22.
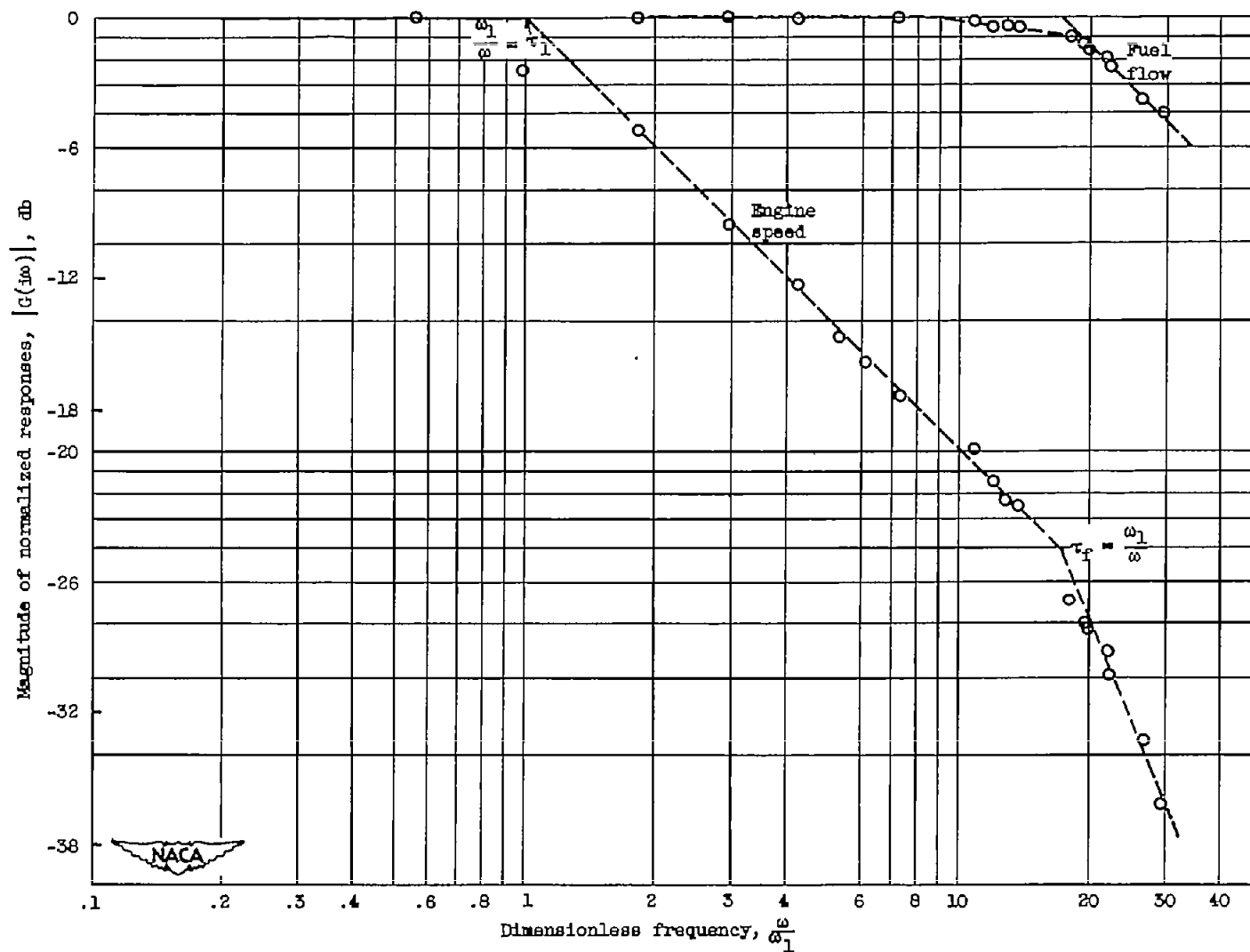
Figure 14. - Frequency spectra of fuel flow and engine speed responses with fuel valve position varying sinusoidally at constant amplitude for turbojet engine operated at simulated altitude of 15,000 feet and simulated flight Mach number of 0.22.
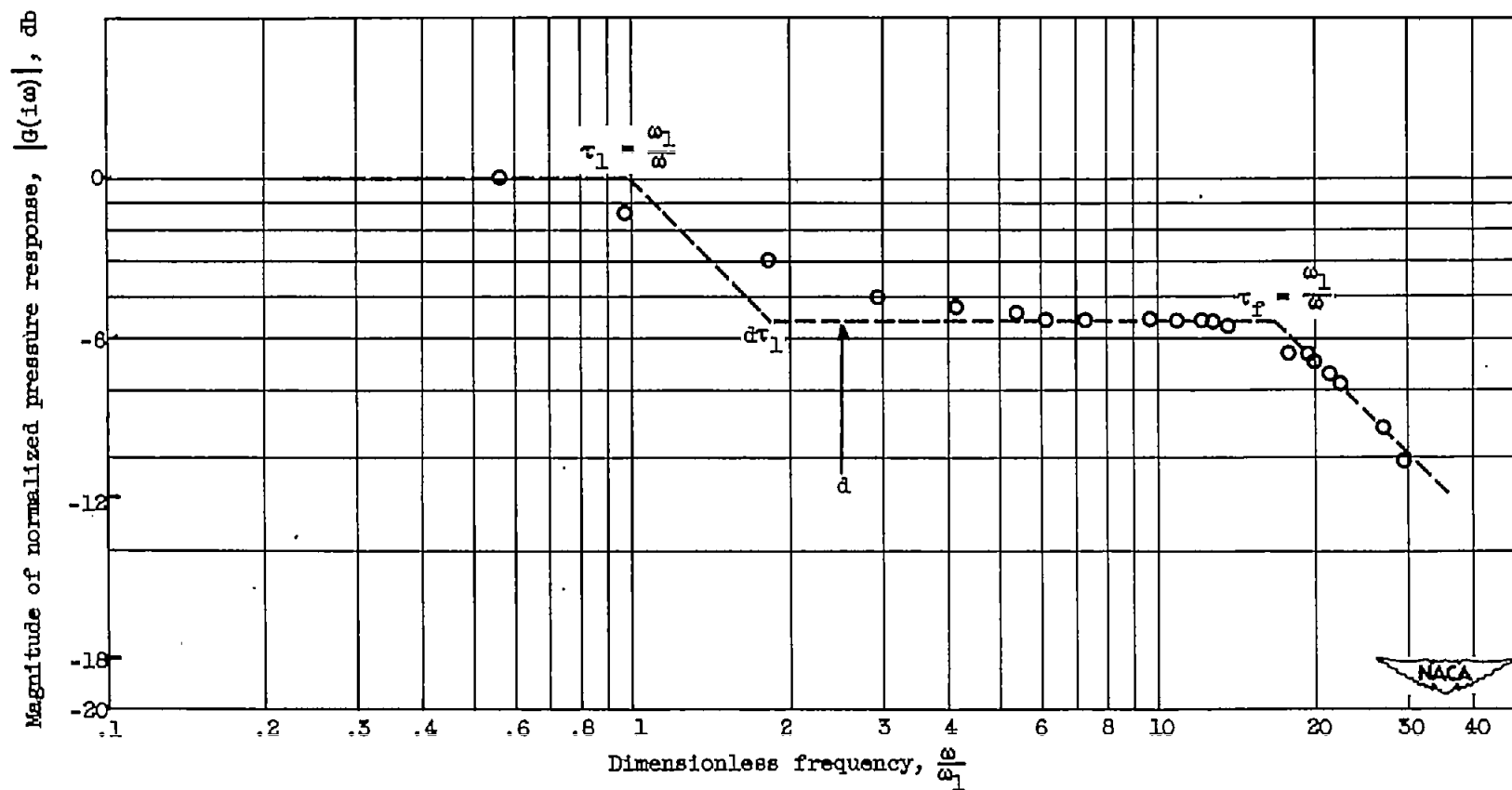
Figure 15. - Frequency spectrum of compressor-discharge total pressure response with fuel valve position varying sinusoidally at constant amplitude for turbojet engine operated at simulated altitude of 15,000 feet and simulated flight Mach number of 0.22.
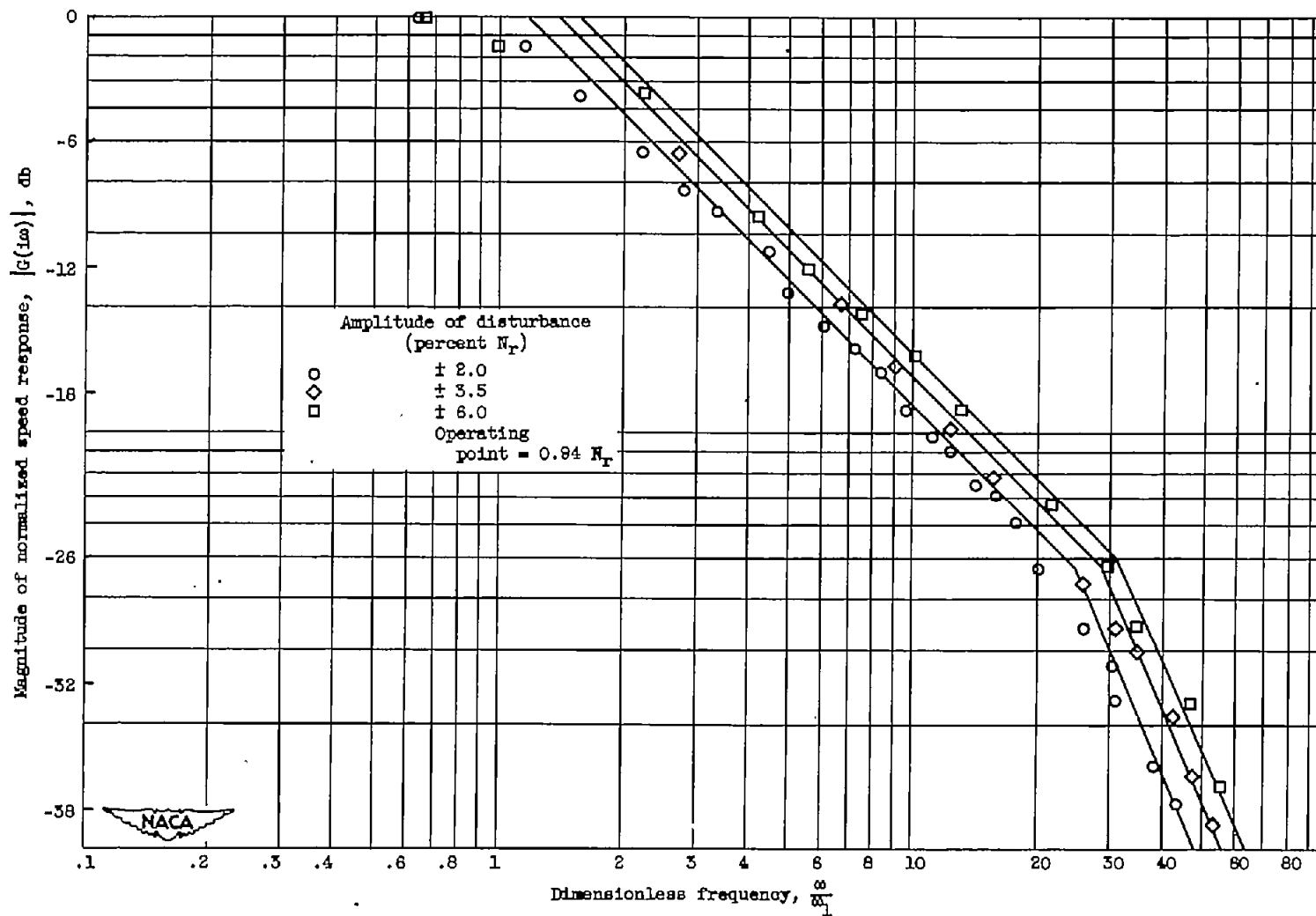
(a) Amplitude ratio.

Figure 16. - Engine speed frequency response to fuel valve position varying sinusoidally at three amplitudes for turbojet engine operated at simulated altitude of 15,000 feet and simulated flight Mach number of 0.22.
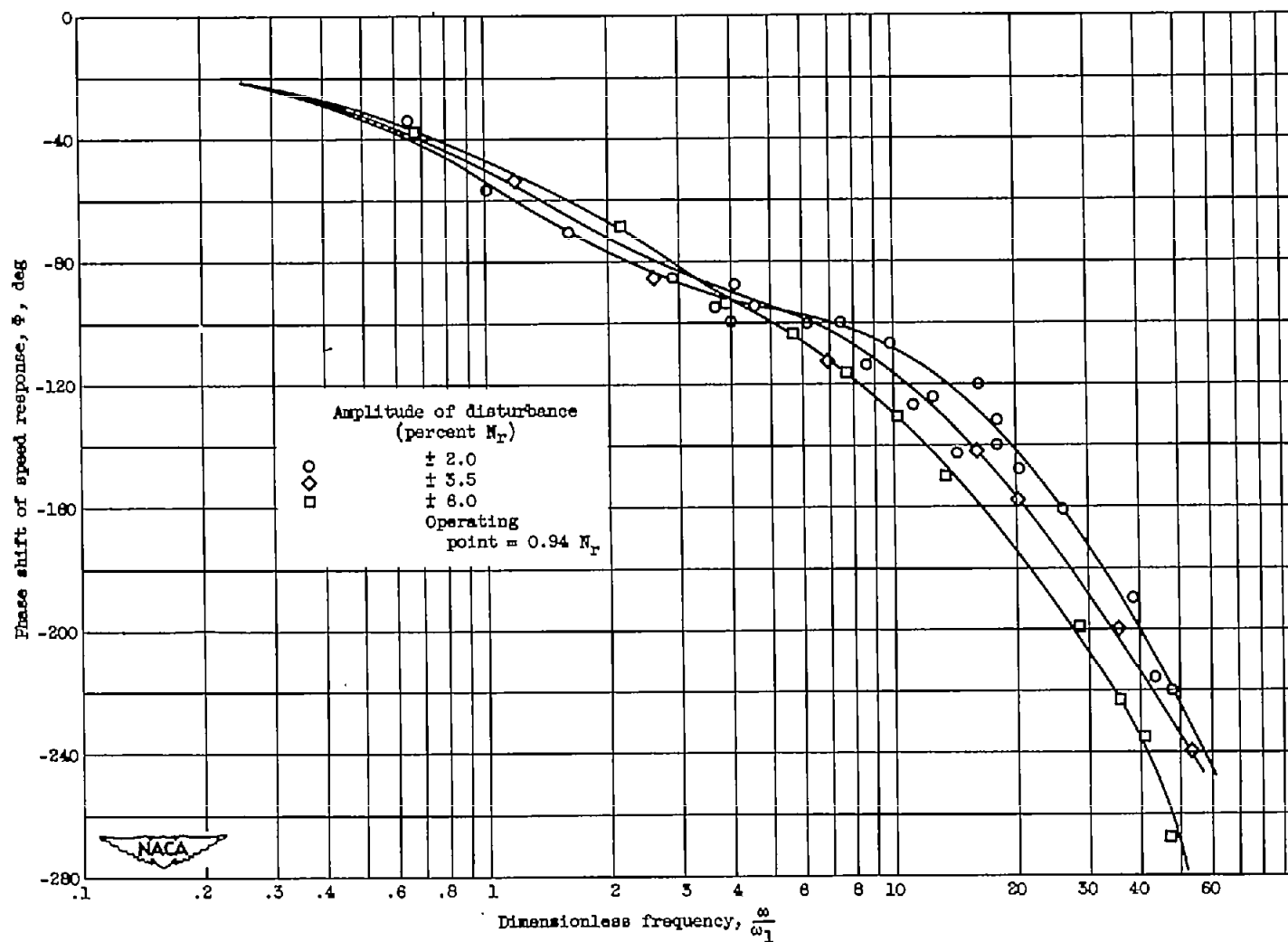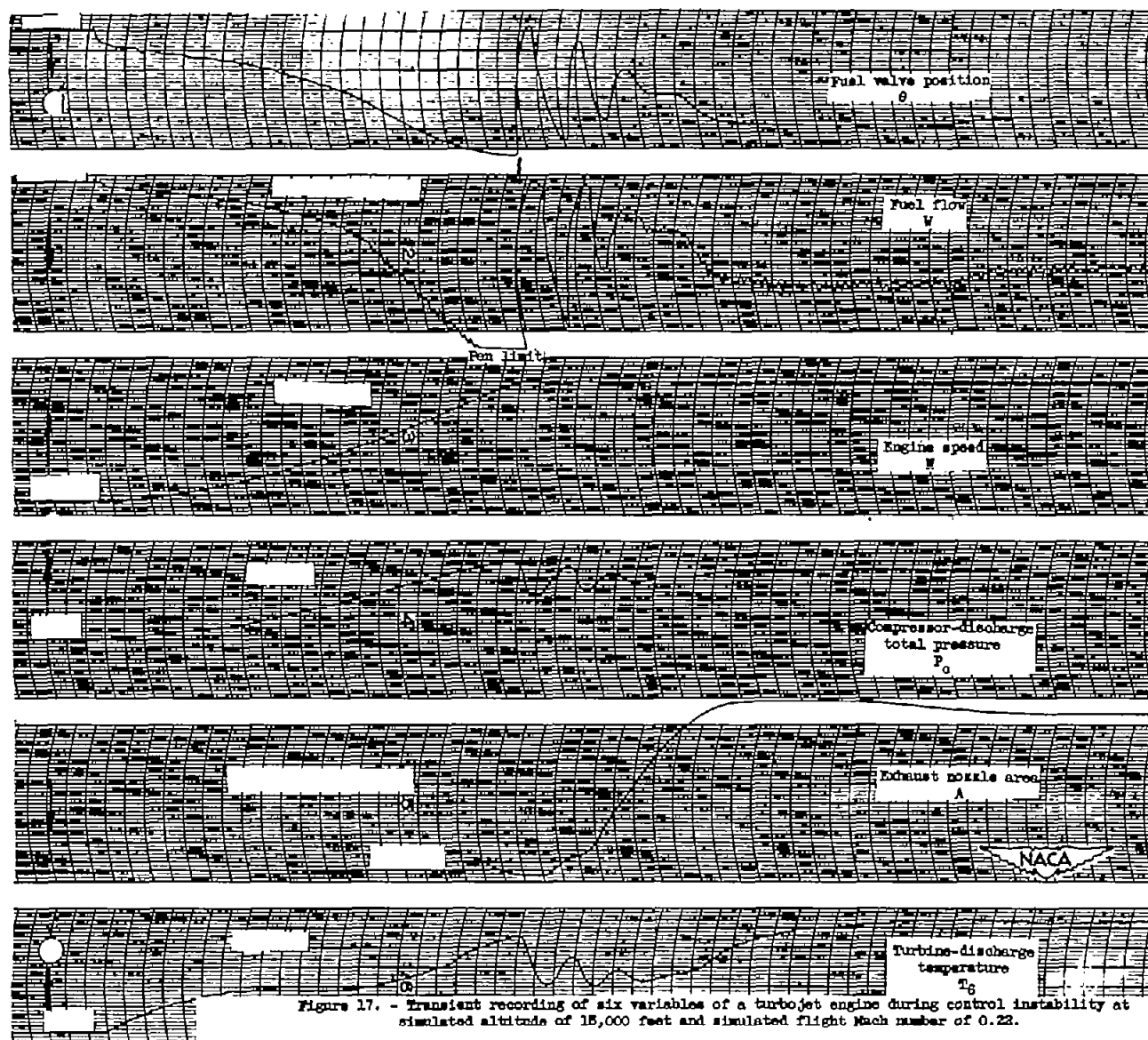
(b) Phase shift.

Figure 16. - Concluded. Engine speed frequency response to fuel valve position varying sinusoidally at three amplitudes for turbojet engine operated at simulated altitude of 15,000 feet and simulated flight Mach number of 0.22.

Fuel valve position
θ

Fuel flow
W

Run limit

Engine speed
N

Compressor-discharge
total pressure
P₃

Exhaust nozzle area
A

NACA

Turbine-discharge
temperature
T₆

Figure 17. - Transient recording of six variables of a turbojet engine during control instability at
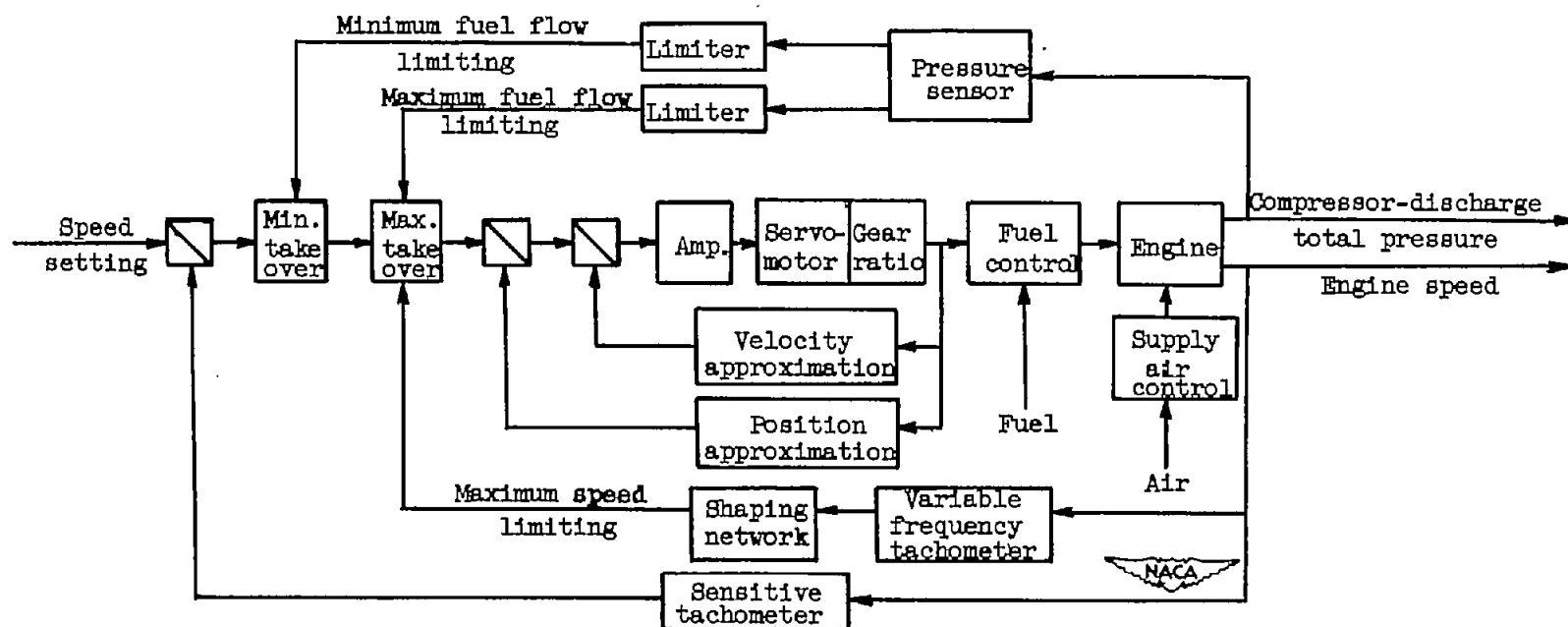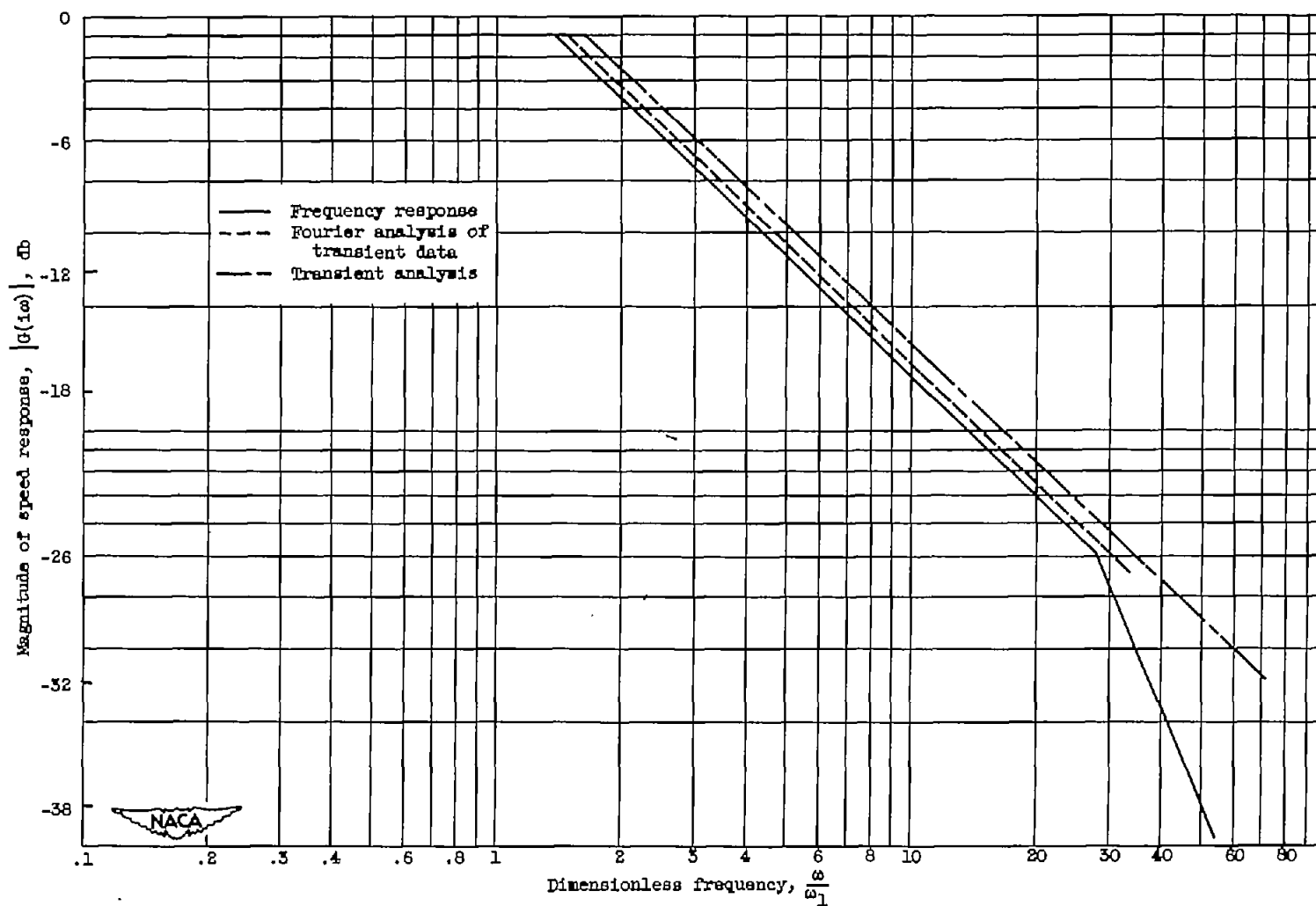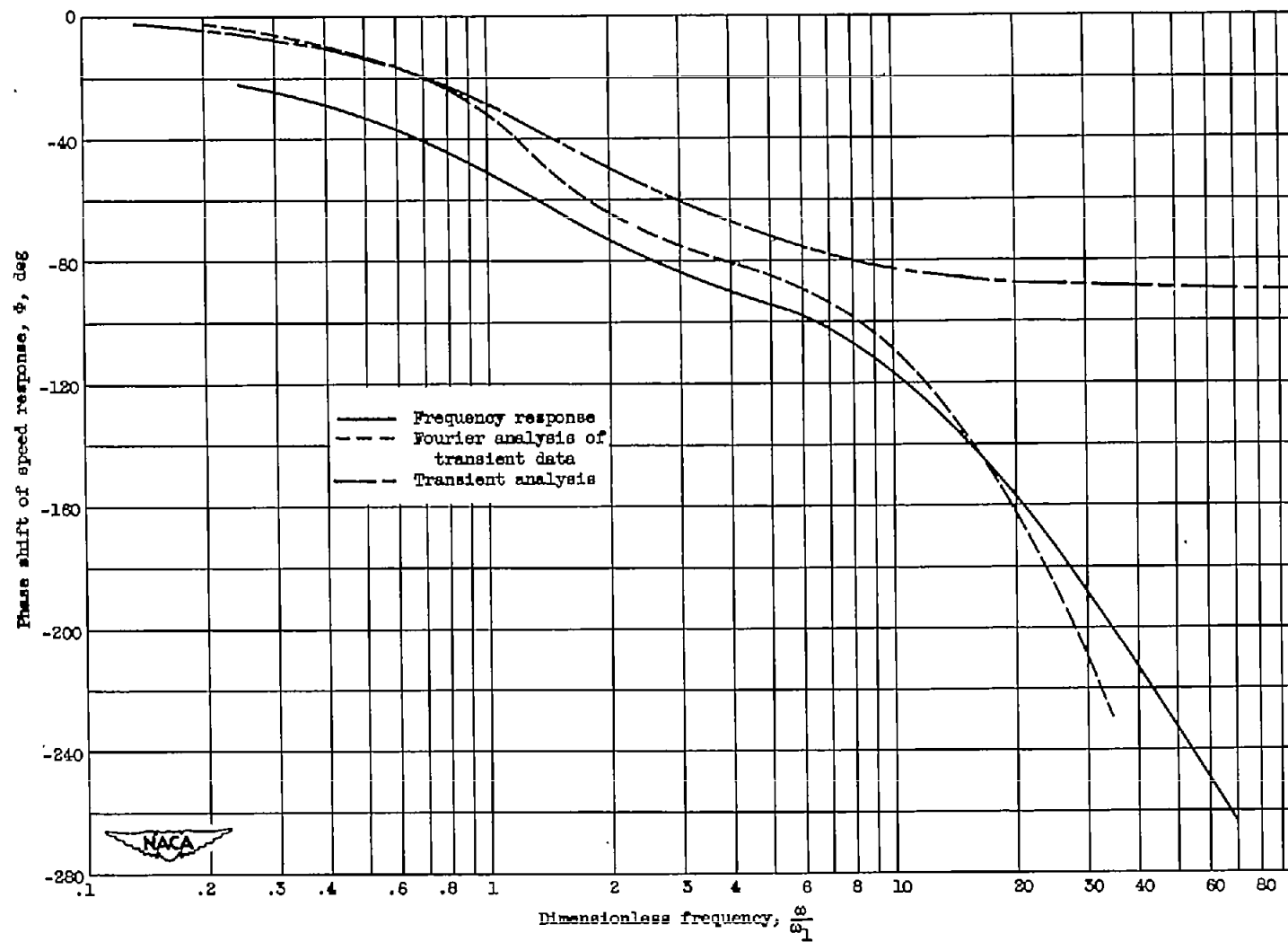simulated altitude of 15,000 feet and simulated flight Mach number of 0.22.

Figure 18. - Block diagram of engine-speed - fuel-flow control loop including limits.

(a) Magnitude.

Figure 19. - Comparison in frequency domain of three methods for determining engine speed response to fuel valve position disturbance for a turbojet engine operating at 0.94 N_r, simulated altitude of 15,000 feet, and simulated flight Mach number of 0.22.

(b) Phase shift.

Figure 19. - Concluded. Comparison in frequency domain of three methods for determining engine speed response to fuel valve position disturbance for a turbojet engine operating at 0.94 N_r, simulated altitude of 15,000 feet, and simulated flight Mach number of 0.22.